รายงานวิจัยฉบับสมบูรณ์

โครงการ

"การเตรียมและตรวจสอบตัวรองรับคะตะลิสต์ที่สังเคราะห์จากสารประกอบอลูมาเทรนและไซลาเทรนโดยวิธีโซล-เจล"

โดย นางสุจิตรา วงศ์เกษมจิตต์

พฤศจิกายน 2545

สัญญาเลขที่ BGJ4380014

รายงานวิจัยฉบับสมบูรณ์

โครงการ

"การเตรียมและตรวจสอบตัวรองรับคะตะลิสต์ที่สังเคราะห์จากสารประกอบอลูมาเทรนและไซลาเทรนโดยวิธีโซล-เจล"

โดย นางสุจิตรา วงศ์เกษมจิตต์

วิทยาลัยปิโตรเลียมและปิโตรเคมี จุฬาลงกรณ์มหาวิทยาลัย

สนับสนุนโดยสำนักงานกองทุนสนับสนุนการวิจัย

กิตติกรรมประกาศ

ผู้วิจัยขอขอบพระคุณสำนักงานกองทุนสนับสนุนการวิจัย ที่ได้ให้การสนับสนุนโครงการวิจัยนี้ตลอดทั้งโครงการ

บทคัดย่อ

รหัสโครงการ : BGJ4380014

ชื่อโครงการ : "การเตรียมและตรวจสอบตัวรองรับคะตะลิสต์ที่สังเคราะห์จากสารประกอบอลูมาเทรนและไซลาเทรนโดยวิธีโซล-เจล"

ชื่อนักวิจัย : นางสุจิตรา วงศ์เกษมจิตต์
วิทยาลัยปิโตรเลียมและปิโตรเคมี จุฬาลงกรณ์มหาวิทยาลัย

E-mail Address : dsujitra@chula.ac.th

ระยะเวลาโครงการ : 2 ปี

วัตถุประสงค์ของงานวิจัยนี้ คือ เพื่อศึกษาวิธีการเตรียมตัวรองรับอลูมินาและซิลิกาจากสารประกอบอลูมาเทรนและไซลาเทรน ตามลำดับ โดยวิธีโซล-เจล และตรวจสอบพื้นที่ผิว ปริมาตรรูพรุน และความว่องไวในการทำปฏิกิริยาของตัวรองรับคะตะลิสต์ที่เตรียมได้ เพื่อหวังว่าจะสามารถนำคะตะลิสต์ที่เหมาะสมมาใช้กับตัวรองรับที่เตรียมได้ และนำไปใช้ในอุตสาหกรรมปิโตรเคมี โดยศึกษาปฏิกิริยารีดักชั่นของก๊าซไนตริกออกไซด์ หรือปฏิกิริยาออกซิเดชั่นของก๊าซคาร์บอนออกไซด์ ดังนั้น งานวิจัยนี้ จึงเริ่มจากการสังเคราะห์ประกอบอลูมาเทรนและไซลาเทรน หลังจากตรวจสอบโครงสร้างของประกอบอลูมาเทรนและไซลาเทรนที่สังเคราะห์ได้ ขั้นตอนต่อไป คือ การสังเคราะห์ตัวรองรับอลูมินาและซิลิกาจากสารประกอบอลูมาเทรนและไซลาเทรน ตามลำดับ โดยผ่านกระบวนการโซล-เจล ซึ่งพบว่า อลูมินาและซิลิกาที่ได้จากการผ่านกระบวนการโซล-เจลมีสมบัติของความเป็นรูพรุนในกลุ่มของเมโซพอรัส และมีพื้นที่ผิวค่อนข้างสูงสมบัติเหล่านี้สามารถนำไปศึกษาต่อโดยใช้เป็นตัวรองรับคะตะลิสต์ให้กับคะตะลิสต์ที่เหมาะสมได้

คำหลัก : ตัวรองรับคะตะลิสต์ สารประกอบไซลาเทรน สารประกอบอลูมาเทรน อลูมินา ซิลิกา และ โซล-เจล

Abstract

Project Code : BGJ4380014

Project Title : "Preparation and Characterization of Catalyst Supports Synthesized from Silatrane and Alumatrane via Sol-Gel Method"

Investigator : Ms. Sujitra Wongkasemjit
The Petroleum and Petrochemical College, Chulalongkorn University

E-mail Address : dsujitra@chula.ac.th

Project Period : 2 Years

The objectives of this research work is to study the synthetic method and properties of catalyst support alumina and silica from alumatrane and silatrane, respectively, via the sol-gel method to hopefully be able to be used with a suitable catalyst needed in petrochemical industries. Therefore, this work was started with the synthesis of alumatrane and silatrane compounds followed by their structural identification. Next step is to synthesize alumina and silica via the sol-gel process. It was found that those synthesized alumina and silica gave homogeneous mesoporous property with high surface area. These properties catalytically are attractive and should be further studied.

Key words : Catalyst support, Silatrane, Alumatrane, Silica, Alumina and Sol-gel process

Table Content

CHAPTER I

INTRODUCTION

Metallatranes, or simply atranes, are intramolecular complex cyclic ester or alkoxides of tris(2-hydroxyalkyl)amines having a skeleton of general structure I.

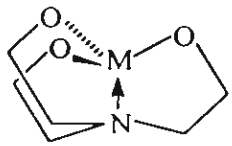

I

where M is an n-valent element having inorganic or organic substituents when n>3. The term metallatranes, proposed by VORONKOV and ZELCHAN in 1965, is an abbreviation used for aminotrialkoxy derivatives of different elements that contain the above skeleton (I). For example, amino-trialkoxyphosphoranes, aminotrialkoxyboranes and aminotrialkoxysilanes give phosphatranes, boratranes and silatranes, respectively. Atrane structures are generally characterized by the tricyclic model having a transannular M←N bond assumed to be present.

Metallatranes with M = B, Al, Si, Ge, Sn, Pb, P, Ti, V, Mo, etc. have been synthesized and studied during the last three decades [VORONKOV et al., (1968); BRADLEY et al., (1978)]. These compounds are of interest because of their cage structure, physical/chemical properties, and especially biological activity.

1.1 Alumatrane

The behavior of monomer A and oligomeric alumatrane has been described previously [HEIN and ALBERT (1952); MEHROTRA (1962); SHKLOVER et al., (1984); BRADLEY et al., (1978); VORONKOV and BARYSHOK (1982); MEHROTRA and RAI (1991)]. In benzene solution, cryoscopy [HEIN and ALBERT (1952)] and ebullioscopy [MEHROTRA (1962)] indicate octameric and hexameric behaviors. A mass spectroscopic (EI 70 eV) study [MEHROTRA (1962)] showed the stability of the dimer B in the gas phase.

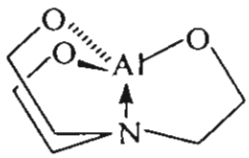

A

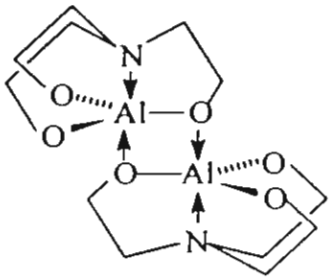

B

There are several methods to prepare alumatranes. The simplest alumatrane was prepared in high yield by the reaction of aluminum alkoxide with triethanolamine in an aromatic solvent (benzene [MEHROTRA (1962)], toluene [THOMAS et al., (1961)]) or with no solvent [HEIN et al., (1952); ICKEN et al., (1964); STANLEY (1968); ELBING et al., (1964)] according to eq 1.1

$$n\ Al(OR)_3 + (HOCH_2CH_2)_3N \longrightarrow \left[Al(OCH_2CH_2)_3N\right]_n + 3n\ ROH \qquad (1.1)$$

Triethylaluminum also reacts with triethanolamine in toluene or hexane at -78°C to form alumatrane [HIGASHI et al., (1968)] see eq. 1.2

$$n\ Al(C_2H_5)_3 + n\ (HOCH_2CH_2)_3N \longrightarrow \left[Al(OCH_2CH_2)_3N\right]_n + 3n\ C_2H_6 \qquad (1.2)$$

VERKADE et al., (1993) used the alcoholysis of tris-(dimethylamido) aluminum with triethanolamine (eq 1.3) and also the transligation of monomeric and dimeric alumaazatranes with triethanolamine (Scheme 1.1)

$$Al(NMe_2)_3 + (HOCH_2CH_2)_3N \longrightarrow \left[Al(OCH_2CH_2)_3N\right]_n + 3MeNH \qquad (1.3)$$

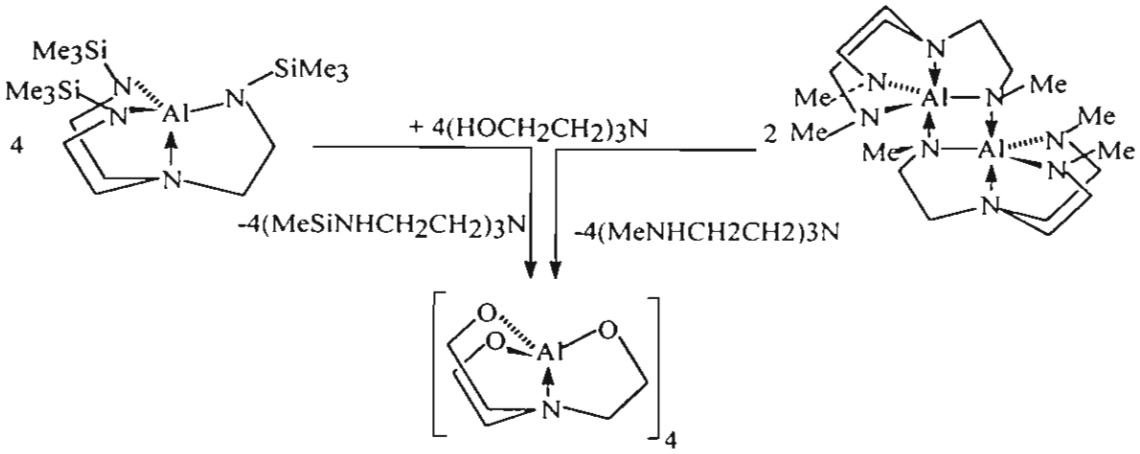

Scheme 1.1

According to ^{27}Al-, ^{1}H-, and ^{13}C-NMR data, they found tetramers in solution and mass spectra revealed the stable tetramer (Scheme 1.2) in the gas phase.

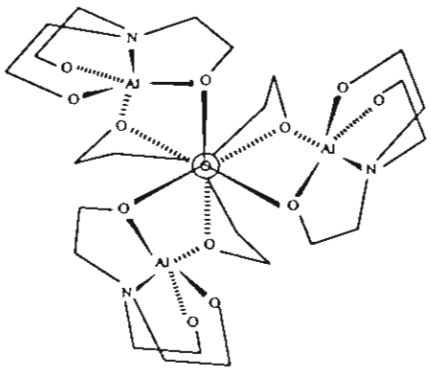

Scheme 1.2

1.2 Silatrane

The first silatranes complexes, C (with X = C_6H_5 and C_2H_5O), were patented by Finestone in 1960, who at that time suggested the existence of the Si←N transannular dative bond in the silatrane molecule synthesized (Finestone A. B., 1960). In 1961, Frye, Vogel, and Hall reported a number of new, 1-substituted silatrane, C [X = H, CH_3, n-$C_{18}H_{37}$, $C_6H_5(CH_3)CH$ and etc.].

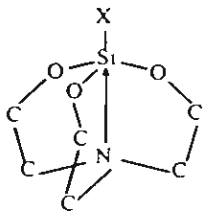

C

They described the 1-ethoxy and 1-phenylsilatranes (melting points = 100°-102°C and 208°-209°C, respectively) and reported some data in support of intramolecular transannular dative bonds in silatrane complexes.

Rosenheim et. al. (Rosenheim A., 1931) reported that silica, sand, and quartz powder could also be employed to react with alkali catecholates to give hexacoordinate silicate complexes. However, Corriu's group demonstrated that these catechol silicate complexes were quite unstable. They could only be modified usefully by reacting with strong nucleophile to obtain tri- and tetrasubstituted products, which were necessary in industry primarily for polymer synthesis, as shown in scheme 1.3 (Corriu R. J. P., 1988).

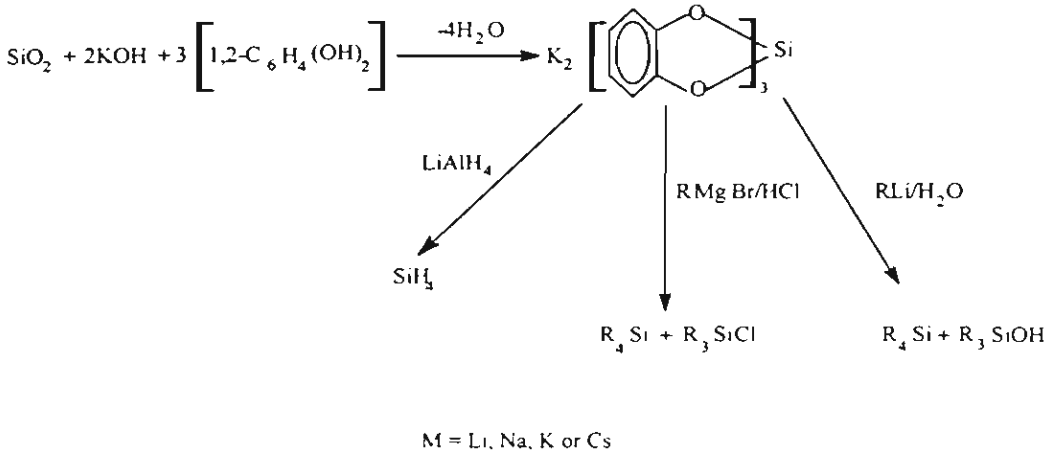

Scheme 1.3

Frye's obervation (Frye C. L., 1970 : 1971) indicated that spirosilicates could react with MeOH and amine base (e.g. Et_3N) to form pentacoordinate, anionic silicate with ammonium counterion at ambient temperature. These species were not stable above 100°C, reverting to the tetracoordinate spirosilicate, as shown in scheme 1.4.

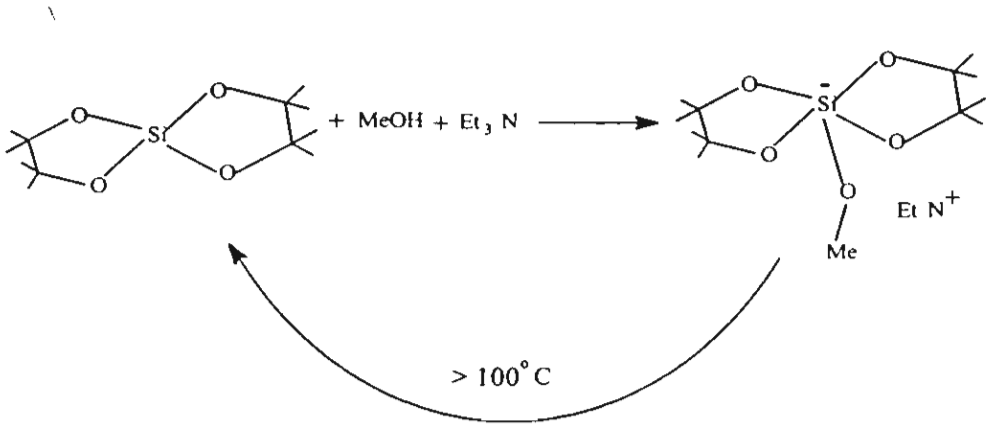

Scheme 1.4

1.3 Sol-gel Process

Basically the sol-gel process means the synthesis of an inorganic network by a chemical reaction in solution at low temperature. The most obvious feature of this reaction is the transition from a liquid (solution or colloidal solution) into a solid (di-or multiphasic gel) led to the expression of "sol-gel process".

Sol-gel chemistry is based on inorganic polymerization reactions starting from molecular precursors, such as metal alkoxides, an oxide network is obtained via inorganic polymerization reactions. Initiation is performed through the hydroxylation of metal alkoxides which occurs upon the hydrolysis of alkoxy groups, as followed in equation 1.4.

$$M\text{-}OR + H_2O \longrightarrow M\text{-}OH + ROH \qquad (1.4)$$

As soon as hydroxyl groups are generated, propagation occurs through a polycondensation process. Depending on experimental conditions, two competitive mechanisms have to be considered. They can be described as follows:

1. Olation : formation of hydroxo bridges through the elimination of solvent molecules, see equation 1.5.

$$M\text{-}OH + M\text{-}O\text{-}\overset{X}{\overset{|}{H}} \longrightarrow M\text{-}O\text{-}\overset{H}{\overset{|}{M}} + X\text{-}OH \qquad (1.5)$$

(X = H or alkyl group)

2. Oxolation : formation of oxygen bridges through the elimination of H_2O or XOH, as shown in equation 1.6.

$$M\text{-}OH + MO\text{-}X \longrightarrow M\text{-}O\text{-}M + X\text{-}OH \qquad (1.6)$$

These three reactions (hydrolysis, olation and oxolation) can be involved in the transformation a metal alkoxide precursor into an oxide network. The structure and the morphology of the resulting network strongly depend on the relative contribution of them. These reactions can be described as nucleophilic substitutions which depend on the nucleophilic group (H_2O, OH-, HO-M), the leaving group (ROH, H_2O) and the metal atom (Si, Ti, Zr, etc.).

One property of the sol-gel process is the ability to control the process all the way, from the molecular precursor to the product. Sol-gel chemistry offers many advantages, such as a lower processing temperature allowing the synthesis of metastable oxides phases and opening a field of opportunity for the synthesis of new materials including both organic and inorganic components. The rheological properties of sols and gels allow fibers or films to be processed by techniques, such as spin-drawing, dip-coating or screen-printing.

Generally, sol-gel process relatively involves 4 following steps:

- Solution chemistry (gel formation)
- Aging
- Drying
- Calcination/Sintering

Solution chemistry step: Starting materials (metal salt or metal alkoxides) are dissolved in an appropriate solvent to form a solution. The gel is hereafter formed in the gelation process, involving simultaneous hydrolysis and polycondensation of metal alkoxide precursor. At this step, the most important parameters are types of precursor, solvent, precursor concentration and temperature.

Aging step:. This step represents the time between the formation of a gel and the removal of solvent. As long as the pore liquid remains in the matrix, a gel can undergo many transformations. For alkoxide derived gels, concentration between surface functional group continues to occur after the gel point. This step can actually be desirable because it leads to a more cross-linked network that is mechanically stronger and easier to handle.

Drying step: It is a process of evaporating solvent from a gel network. Similarly to aging, a gel is not static during drying and, for that reason, drying can be viewed as part of the overall aging process. The properties of product are thus dependent on the drying method and condition.

Calcination/Sintering: It often is done in the presence of a reactive gas (e.g. flowing air, oxygen) in order to burn off any residue organics or to oxidize the sample. Exposing the sample to a high temperature over an extended period of time leads to sintering and consequently a decrease in surface area. The process also causes the material to crystallize into different structure forms. Thus, the physical

characteristics of the product depend on parameters, such as temperature, heating rate and gaseous environment.

Fundamentally, the uses of metal alkoxides depend on their chemical reactivity coupled with their volatility and solubility in common organic solvents. The chemical reactivity is manifest in a variety of catalytic applications of the alkoxides, ranging from redox catalyst (aluminium alkoxides in Meerwein-Ponndorf-Verly reactions with those used to synthesize primary alcohol from aldehyde), olefin polymerization catalysts (titanium and vanadium alkoxides as components of Ziegler-Natta catalysts) to accelerators for drying paints and inks. Ultimately, the alkoxides are valuable precursors to the metal oxides through hydrolysis, pyrolysis or combustion. Where high purity is at stake and the metal alkoxides offer considerable advantages as starting materials for the preparation of high purity oxides.

The starting materials to synthesize silicon or aluminium alkoxides are expensive and the syntheses are multistep. LAINE et al. have developed an inexpensive way to convert metal oxides, namely, alumina and silica, into novel materials ranging from ion conducting, liquid crystalline polymers (RAY et al., 1992), to oligomeric and polymeric precursors.

LAINE et al. found that higher boiling point amine bases (b.p.>200°C), such as triethanolamine and triethylenetetramine can be used either in catalytic or stoichiometric quantities to dissolve SiO_2. Moreover, they also found that approximately stoichiometric quantities of TEA will effectively dissolve $Al(OH)_3$. The "Oxide One Pot Synthesis Process (OOPS)" for alkoxyalanes was developed after it was discovered that stoichiometric amounts of TEA would dissolve aluminum hydroxide, the source material for most pure alumina [KIRK-OTHEMER (1979); COTTON and WILKINSON (1967)].

This research work was aimed at the synthesis and characterization of silica and alumina directly from silatrane and alumatrane complexes via the sol-gel process.

References

Alberty R. A. and Silbey R. J., *Physical Chemistry*, John Wiley & sons, Inc., Singapore, 547-710, 1955

Bradley, D. C., Mehrotra, R. C., Gaur, D. P., *Metal Alkoxides;* Academic Press: N. Y., 1978, 266.

Cotton, F. A. and Wilkinson, G. F., *Advanced Inorganic Chemistry*, John Wiley&sons, Interscience Pulb., N.Y., 1981.

Corriu R. J. P., *Pure and Appl. Chem.*, 60, 99-160, 1988

Elbing, I. N. and Finestone, A. B., *German offen 1.*, 1964, 1,162,439; *Chem. Abstr.*, 1964, 60, 17/4705.

Finestone A. B., *US* 2, 953, 545, 1960

Frye C. L., *Ibid* 93, 6805-6810, 1971

Frye C. L., *J. Am. Chem. Soc.*, 92, 1205-1210, 1970

Frye C. L., Vogel G. E., Hall J. A., *J.Am.Chem. Soc.*, 83, 996, 1961

Hein, F. and Albert, P. W. Z., *Anorg. Allg. Chem.*, 1952, 269, 67.

Higashi, H. and Namikawa, S., *Kogyo Kagaku Zasshi*, 1967, 70,97.

Icken, J. M. and Jahren, E. J., *Belg. Patent 619*, 1963, 940; *Chem. Abstr.*, 1963, 60, 2768.

Kirk-Othemer, *Encyclopedia of Chemical Technology*, third edition, Wiley-Interscience Publ., N.Y., 1979, 2, 129-262.

Laine R. M., *NATURE*, 353, 1991

Mehrontra, R. C. and Mehrotra, R K., *J. Indian Chem. Soc* , 1962, 39, 677.

Mehrotra and Rai, A. K., *Polyhedron*, 1991, 10, 1967.

Ray, D. G., Laine, R. M., Robinson, T. R., Vincy, C., *Mol. Crys. Liq. Crystal*, 1992, 225,153.

Rosenheim A., Raibmann B and Schendel, G.Z., *Anorg. Allg. Chem*, 160. 196, 1931

Shklover, V. E., Struchkov, Yu. T., Voronkov, M. G., Ovchinnikova, Z. A. and Baryshok, V. P., *Dokl. Akas. Nauk (Engl. Transl)*, 1984, 227, 723.

Stanley, R. H., *British Patent 1*, 1968, 123,559; *Chem. Abstr.*, 1968, 69, 78532.

Thomas, W. M., Groszos, S. J and Day, N. E., *U.S. Patent 2,* 1961, 985, 685; *Chem. Abstr.,* 1961, 55, 20966.

Verkade, J. K., *Acc. Chem. Res.,* 1993, 26, 483.

Voronkov, M. G., *Vestnik Akad. Nauk SSSR,* 1968, 38, 48

Voronkov, M. G. and Baryshok, V. P., *Organomet. Chem.,* 1982, 239, 199.

Voronkov, M. G. and Zelchan, G. I., *Khim. geterotsikl. soed.,* 1965, 51.

CHAPTER II
SYNTHESIS OF SILATRANE

ABSTRACT

New convenient and inexpensive method of tris(silatranyloxy-*i*-propyl)amine synthesis directly from silica and triisopropanolamine (TIS) has been elaborated using ethylene glycol solvent. The silatrane product is obtained in one step via the "Oxide One Pot Synthesis (OOPS)" process. In the presence of catalytic amounts of triethylenetetramine (TETA), the reaction easily takes place. The product is characterized using DSC, TGA, ^{1}H-, ^{13}C-, ^{29}Si-NMR and FAB^{+}-MS. The FTIR result indicates the presence of N⟶Si transannular bonding. The chemical and physical properties of these compounds are described specially with respect to their polymeric properties.

INTRODUCTION

The limited number of simple silicon-containing starting materials restricts the potential role of inorganic and organometallic silicon compounds in the development of new chemical reagents, polymeric glasses and ceramics. The reason is that silicon-containing chemicals are almost exclusively prepared from elemental silicon, obtained from the carbothermal reduction of silica at around 1200 °C[1]. The utilization of crude silica to form silicon-containing compounds directly, in order to circumvent this energy-intensive step, has been the aim of a number of research groups by a variety of strategies.

Silatranes, for example, as a class of pentacoordinated silicon compounds are known for more than three decades, and their specific biological[2-3], physico-chemical[4-5] and structural[6-7] properties still attract research interests. Although the investigation results were published in many papers[8-10], most of them deal solely with the intriguing property study of these compounds.

The most popular methods for the silatrane synthesis are the reactions of halo-, hydro- and alkoxysilanes with triethanolamine or its derivatives[11](see eq.2.1). The original way of silatrane synthesis from ethoxysilanes and boratrane in the presence of $Al(O\textit{i}\text{-}Pr)_3$ or Al_2Cl_6 has also been described[12-13].

$$XSi(OC_2H_5)_3 + (HOCH_2CH_2)_3N \longrightarrow XSi(HOCH_2CH_2)_3N + 3C_2H_5OH \quad (2.1)$$

$X = C_2H_5O,\ C_6H_5$

Recently, Laine and colleagues have found a way to synthesize organosilicon compounds directly from inexpensively starting material, silica (SiO_2), and ethylene glycol in only one step[14-16]. They also found a way to synthesize tris(silatranyloxyethyl)amine from silica and triethanolamine[17] via the "OOPS" process, as shown in eq.2.2.

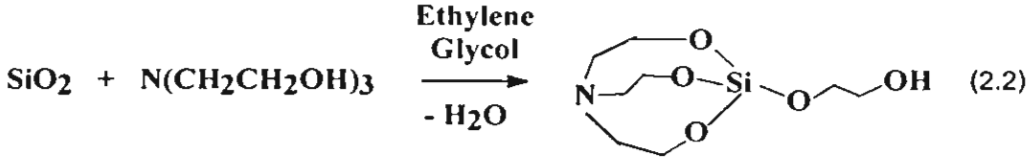

(2.2)

We have been further investigating this reaction with different kind of trialkoxylamine, namely TIS, to determine whether similar silatrane product can be obtained. This paper describes the production and characterization of tris(silatranyloxy-*i*-propyl)amine via the "OOPS" process directly from silica, which is a widespread and inexpensive starting material, as compared to triethoxysilanes which are far more expensive, and TIS.

EXPERIMENT

Materials

All reactions were carried out under a N_2 atmosphere with careful exclusion of extraneous moisture and air since the product is slightly sensitive to moisture and air. The glassware used for these experiments was oven dried. Amorphous, precipitated silicon dioxide, SiO_2, with a multi-point BET surface area of 182 m^2/g, was donated by PPG Siam Silica Co., Ltd. and used as received. It was stored in a dry environment prior to use to prevent moisture adsorption. Ethylene glycol, EG, (99.5% Farmitalia Carlo Erba) used as solvent in the reaction was distilled before used by fractional distillations at 200 ^{o}C. Triethylenetetramine, TETA, (Union Carbide, Thailand, Ltd.) used as a base catalyst was distilled under vacuum prior to use. TIS was obtained from Fluka Chemika Company and used as received. Anhydrous diethyl ether and dichloromethane (J.T. Baker Inc.) used as purification solvents were purified by standard techniques under N_2 atmosphere. Dichloromethane was distilled from anhydrous calcium chloride, and anhydrous diethyl ether was dried by adding anhydrous calcium chloride and kept in a clear dry Winchester bottle.

Characterization

FTIR spectra were obtained using a Bio-Rad FT-45A spectrometer with a resolution of 4 cm^{-1}. A solid sample was thoroughly ground using 1% of sample to 99% by weight of pure and dry crystalline KBr, followed by mixing and pressing hydraulically into pellet. ^{1}H-, ^{13}C-, ^{29}Si-NMR spectra were obtained using a 500 MHz JEOL spectrometer at room temperature in DMSO-d_6 as solvent and TMS as

internal reference. Mass spectra were obtained on a Fison Instrument (VG Autospec-ultima 707E) with VG data system using a direct probe of the positive fast atom bombardment technique (FAB^+ mode) and cesium iodide (CsI) as a standard for peak calibration.

Thermal transition properties were determined using a Netzsch DSC 200 at a heating rate of 10°C /min under nitrogen atmosphere. The thermal stability of the synthesized products was obtained using Netzsch TGA 209 at a heating rate and flow rate of 20°C and 10 mL per min., respectively.

Synthetic Method

Synthesis of silatrane complex was carried out with and without catalyst TETA by placing 6.09g. (100 mmol) of silica, 19.12 g. (100 mmol) of TIS, and 100 mL of ethylene glycol into a 250 mL two-neck reaction flask. In case of running the reaction with catalyst, then 0.15 g. (1 mmol) of TETA was also added into the mixture. The solution mixture was magnetically stirred and heated to the boiling point of EG under N_2 atmosphere to distill off EG and by-product, water. During the course of reaction, the same amount of fresh EG as distillate was added. This process of EG distillation and addition was repeated until the mixture turned clear, indicating that the reaction was complete which took approximately 5 and 10 h for the reaction containing with and without TETA, respectively. The remaining EG was removed by vacuum distillation (10^{-2} torr) using an oil-bath temperature of 100± 5°C. The resulting product turned very viscously at this point. It was then purified by precipitating with dried 10% dichloromethane in diethyl ether. The powder product was filtered off, dried in vacuum oven at 50°C for 10 h., and finally characterized by TGA, DSC, FAB^+-MS, FTIR and NMR.

RESULTS AND DISCUSSION

Silatrane complex, tris(silatranyloxy-*i*-propyl)amine, (I), was synthesized via the "Oxide One Pot Synthesis (OOPS)" process using widely available SiO_2 in the presence and absence of TETA catalyst under identical conditions. The reaction without TETA took twice longer than the one with TETA. Characterization of isolated products from both reactions indicated that their structures were almost identical, except that the product obtained from the reaction with TETA was bis(silatranyloxy-*i*-propyl)-hydroxyl- *i*-propyl amine, (II), as discussed in detail below.

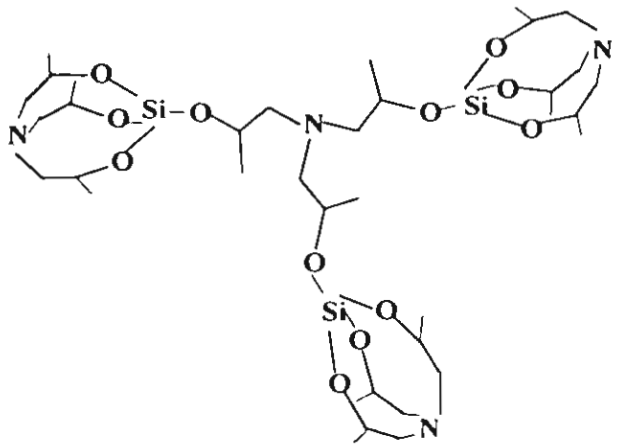

I

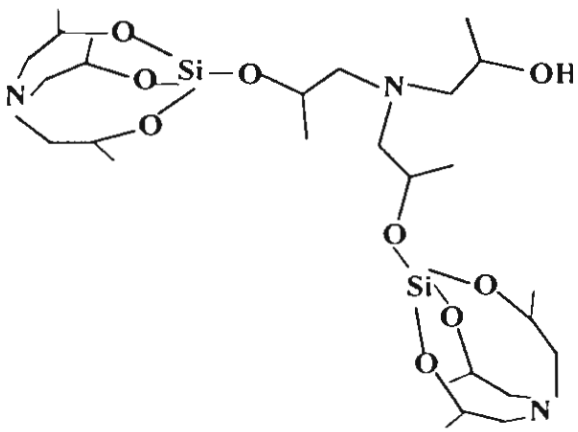

II

Thermogravimetric Analysis (TGA)

The silatrane product without TETA show three regions of mass loss, 150°-250 °C, 290°-370 °C and 390°-620 °C, see Figure 2.1(a). The first one corresponds to the loss of traces of residual EG and TIS. The second and the last mass loss correspond to organic ligand decomposition and the oxidation of residual carbon char, respectively. The final %ceramic yield is 22%, as compared to 21.5% for the theoretical ceramic yield.

In case of the product obtained with TETA (Fig. 2.1(b)), it show similar mass losses to that from the reaction without TETA, except the mass loss between 260°-320 °C. This region is likely belong to the TETA mixed in the product which is supported by NMR data indicating that approximately 15% TETA is present in the product. As a result, the % ceramic yield was only 16%, which is lower than the theoretical ceramic yield, 19.2%.

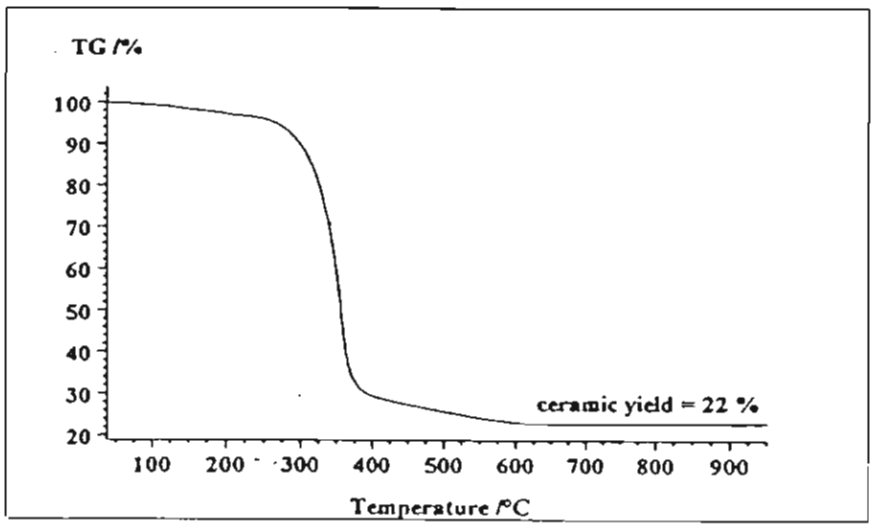

(a)

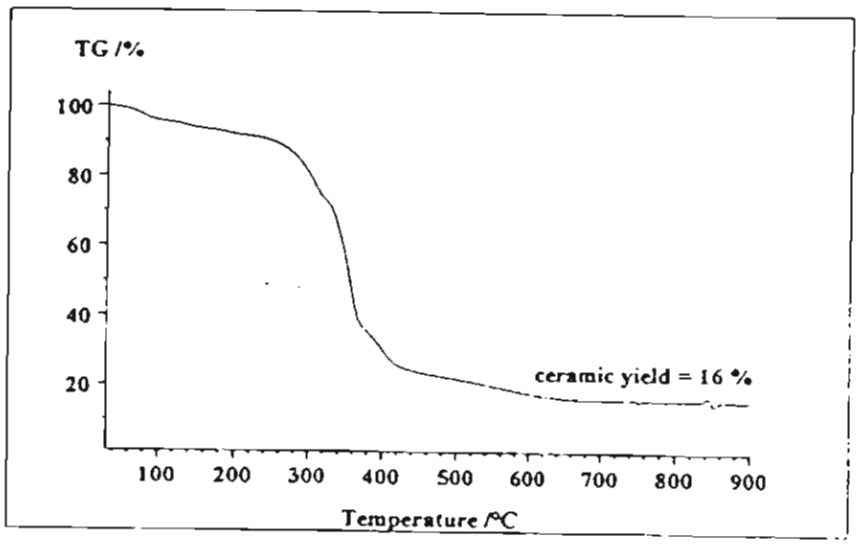

(b)

Figure 2.1 : TGA of Precipitated Silatrane Complexes, (a) without TETA and (b) with TETA

Differential Scanning Calorimeter (DSC)

DSC data of both products (Figure 2.2) show similar results to the TGA profiles. Both exotherms at about 140 °C correspond to decomposition of EG, TIS and TETA. The peaks at 220° and 180 °C in Figures 2.2(a) and 2.2(b), respectively, corresponding to the melting point of silatrane complexes, confirm that using catalyst in a reaction always results in shorter oligomers, as supported by FAB*-MS, than the product obtained from the one without TETA.

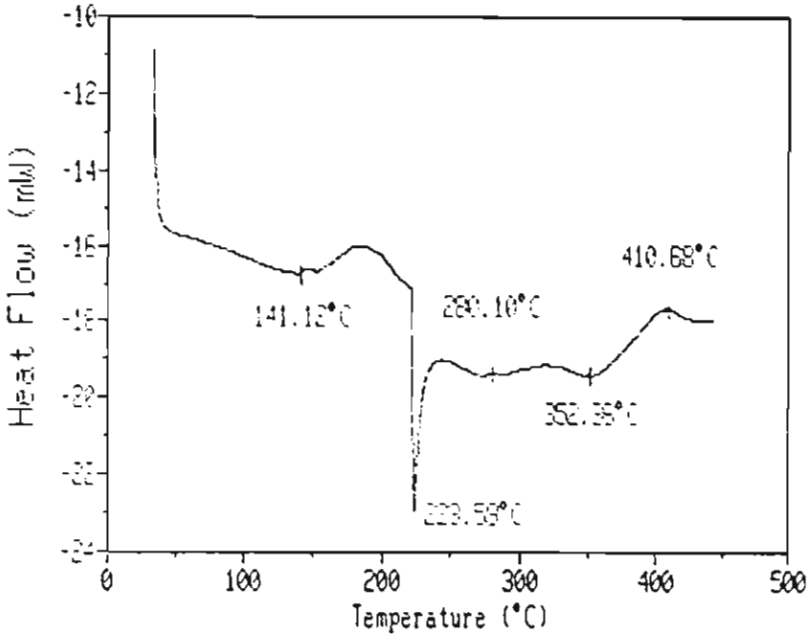

(a)

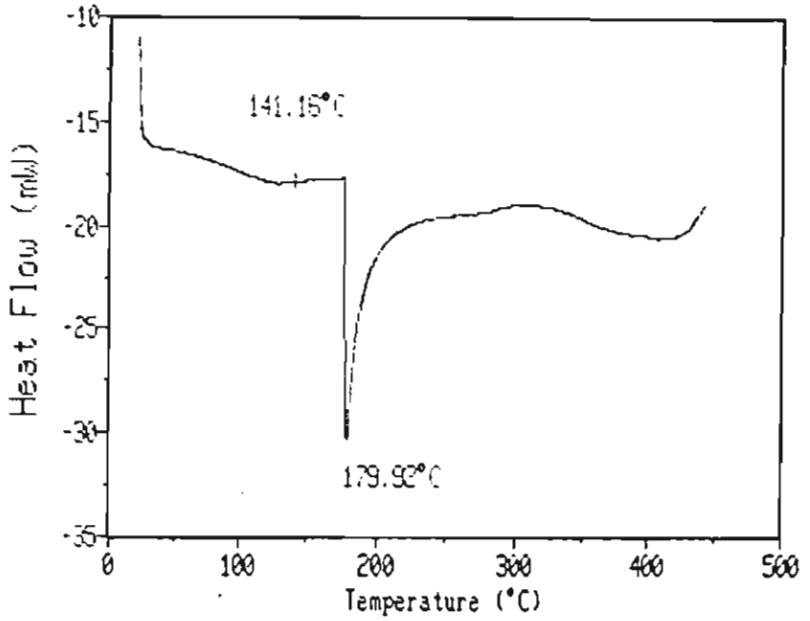

(b)

Figure 2.2 : DSC of Precipitated Silatrane Complexes, (a) without TETA and (b) with TETA

Positive Fast Atom Bombardment Mass Spectroscopy (FAB$^+$-MS)

The FAB$^+$-MS spectrum fragmentation pattern can be employed to confirm the silatrane structures, as can be seen in Table 2.1 showing the proposed structures of the complexes obtained from the reaction without and with TETA. These structures support the fragmentation patterns in Figure 2.3.

Table 2.1: The proposed structures and the pattern of fragmentation of the products obtained from the reactions w/o and w/ TETA

m/e	Intensity		Species
	w/o TETA	w/ TETA	
838 (836 + $2H^{\cdot}$)	8	-	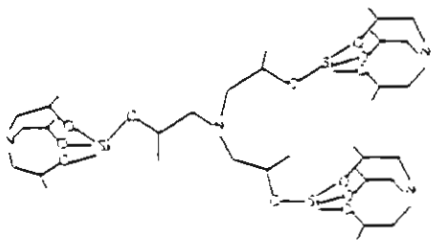
623 (621 + $2H^{\cdot}$)	22	8	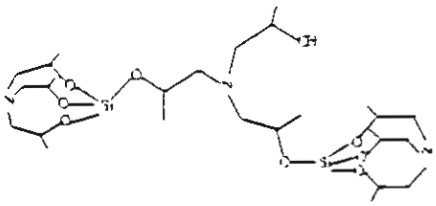
407 (405 + $2H^{\cdot}$)	63	18	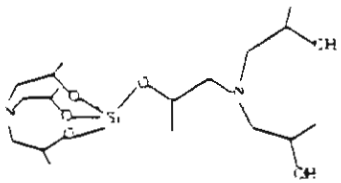
361 (360 + $H^{\cdot}$)	24	10	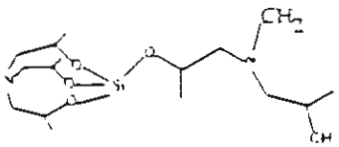
216 (215 + $H^{\cdot}$)	100	100	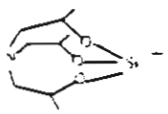

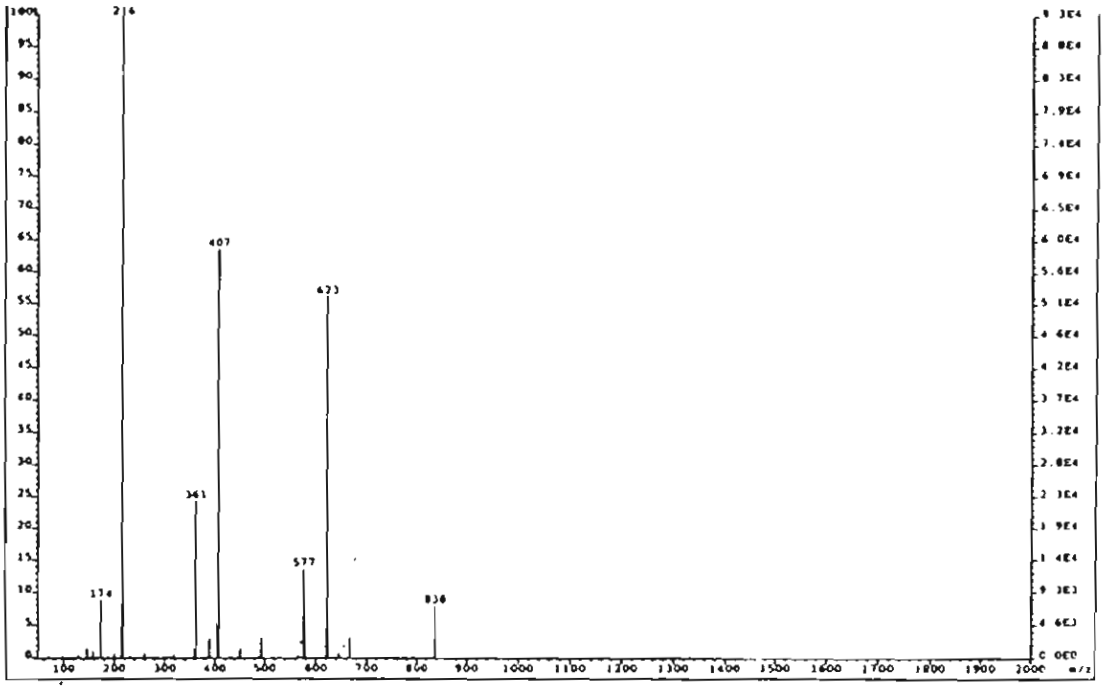

(a)

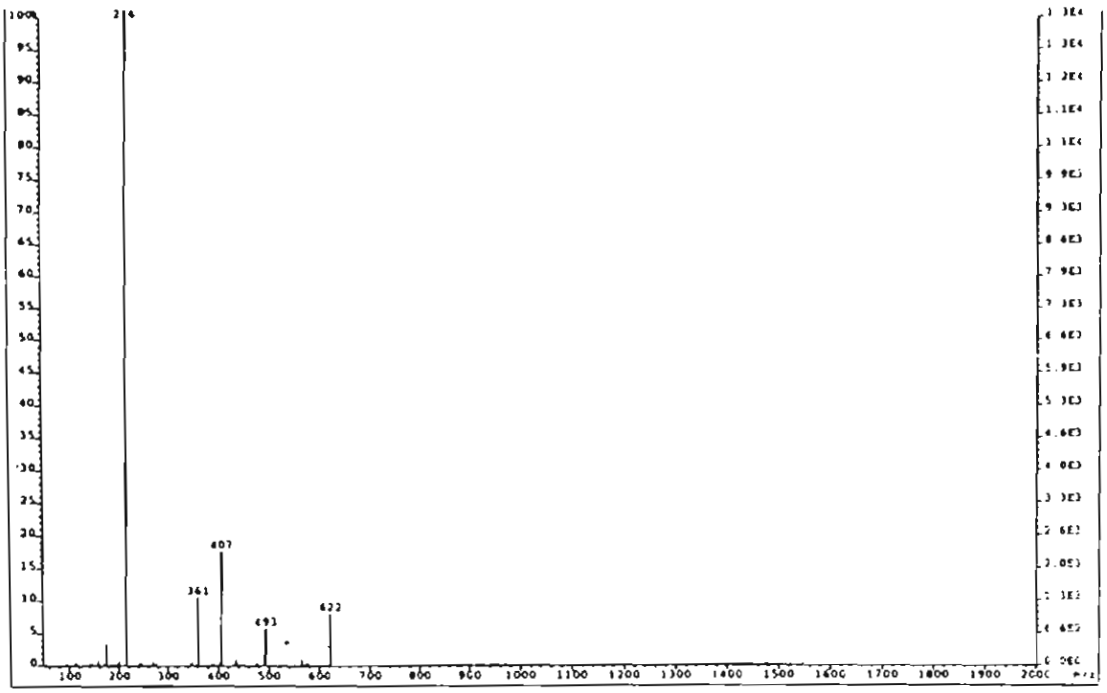

(b)

Figure 2.3 : FAB^{+}-MS Fragmentation Patterns of Silatrane Complexes, (a) without TETA and (b) with TETA

From the results of FAB^{+}-MS spectroscopy, Figure 2.3 and Table 2.1 indicate that the product without TETA mainly consists of the oligomer that has the molecular ion peak at m/e 838, and the base peak is the monomer silatrane. The second highest intensity is the fragment with m/e 407, which has an intensity of 63%.

The fragmentation pattern of the product with TETA is similar to the pattern of the product from the reaction without TETA, except that the m/e 838 is absent. This is probably because TETA acts like an accelerator in the reaction, which results in the shorter chain of oligomers.

Fourier Transform Infrared Spectroscopy (FTIR)

FTIR spectra show that the precipitated product of the reaction with TETA gives the same peaks found in the reaction without TETA. Both products indicate the presence of strong Si-O-C stretching bands at about 1015-1085 cm^{-1}. The peak at 2800-2976 cm^{-1} corresponds to the C-H stretching, whereas the peak at 1380-1460 cm^{-1} is resulted from the C-H bending. The peak at 1270 cm^{-1} comes from the C-N stretching. The strong peak at 1030-1070 cm^{-1} corresponds to the C-O stretching and the peak at 560-590 cm^{-1} refers to the Si←N dative bond.

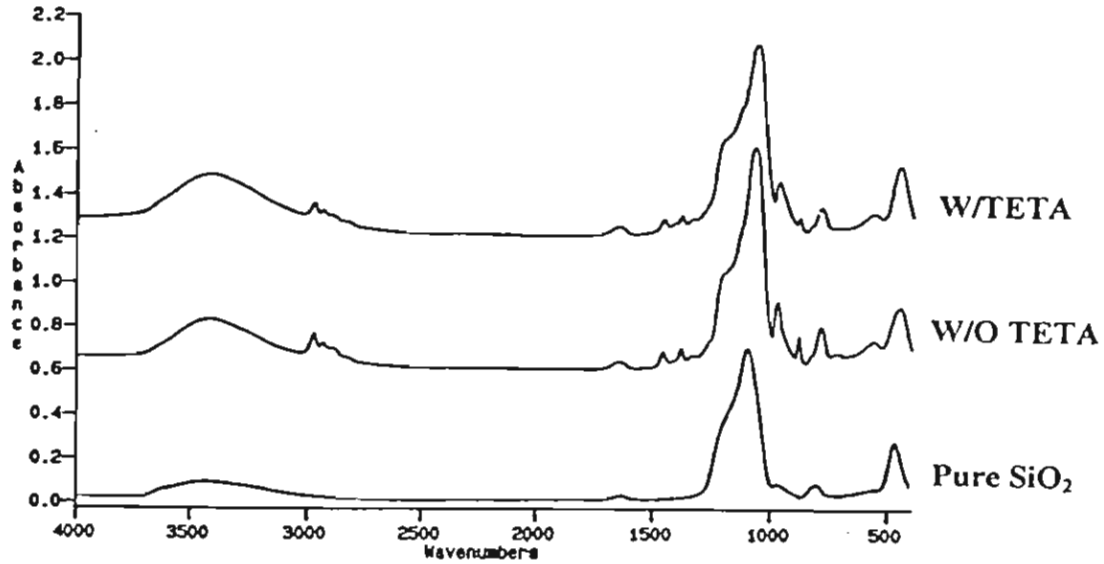

Figure 2.4 : FT-IR Spectra of Pure Silica and Silatrane Complexes w/o and w/ TETA

Nuclear Magnetic Resonance Spectroscopy (NMR)

The ^{1}H-, ^{13}C- and ^{29}Si-NMR spectra are used to confirm the structure of silatrane complexes. For the product without TETA ^{1}H-NMR spectrum in d_6-DMSO shows peaks at 0.96-1.12,

2.86-2.91, 3.3, 3.4-3.5, and 4.0 ppm, which are assigned to CH-C$\underline{H}_3$, N-C$\underline{H}_2$, C$\underline{H}_2$-O, $CH_2O\underline{H}$ of EG, and C$\underline{H}$-CH_3, respectively. The ^{13}C-NMR spectrum shows peaks at 20-21, 23, 57.7, 59.2, and 62.5-65 ppm which can be attributed to H_2C-CH-$\underline{C}H_3$, H_2C-$\underline{C}$H-CH_3, N-$\underline{C}H_2$, $\underline{C}H_2$-O, $\underline{C}H_2OH$ of EG, respectively.

^{1}H- and ^{13}C-NMR spectra of the silatrane complexes with TETA show similar peaks to those obtained from the reaction without TETA, except that ^{1}H-NMR spectrum shows the peaks at 2.6-2.7, which is the group of NH_2-C$\underline{H}_2$ in TETA. ^{13}C-NMR spectrum also shows peaks at 39-41 ppm indicating the NH_2-$\underline{C}H_2$ group of TETA. All results are summarized in Table 2.2.

Table 2.2 : Compared Peak Positions of Products

Position	Groups	^{1}H-NMR (ppm)	^{13}C-NMR (ppm)
a	N-C$\underline{H}_2$	2.86-2.91	57.7
b	C$\underline{H}$-CH_3	4.0	23
c	CH-C$\underline{H}_3$	0.96-1.12	20-21
d	C$\underline{H}_2$-O	3.3	59.2
e	$CH_2O\underline{H}$ of EG	3.4-3.5	62.5-65
f	NH_2-C$\underline{H}_2$ of TETA	2.6-2.7	39-41
g	NH-C$\underline{H}_2$ of TETA	2.9-3.1	60.4-60.7

^{29}Si NMR spectra of precipitated products of the reactions without and with TETA show the peaks at 96 and 98 ppm, respectively, identifying a pentacoordinate Si with dative bond[18], as shown in Figure 2.5. One silica atom is bonded not only with 4 oxygen atoms, but also has a transannular dative bond, which interacts with N atom of TIS. Transannular dative bond is not like a "normal" silicon-nitrogen bond because internuclear distance (r_{Si-N}) is considerably shorter than the vander waal but longer than Si-N covalent bond. This is confirmed by the detailed X-ray crystalliographic studies by Boer and Turley in 1968[19].

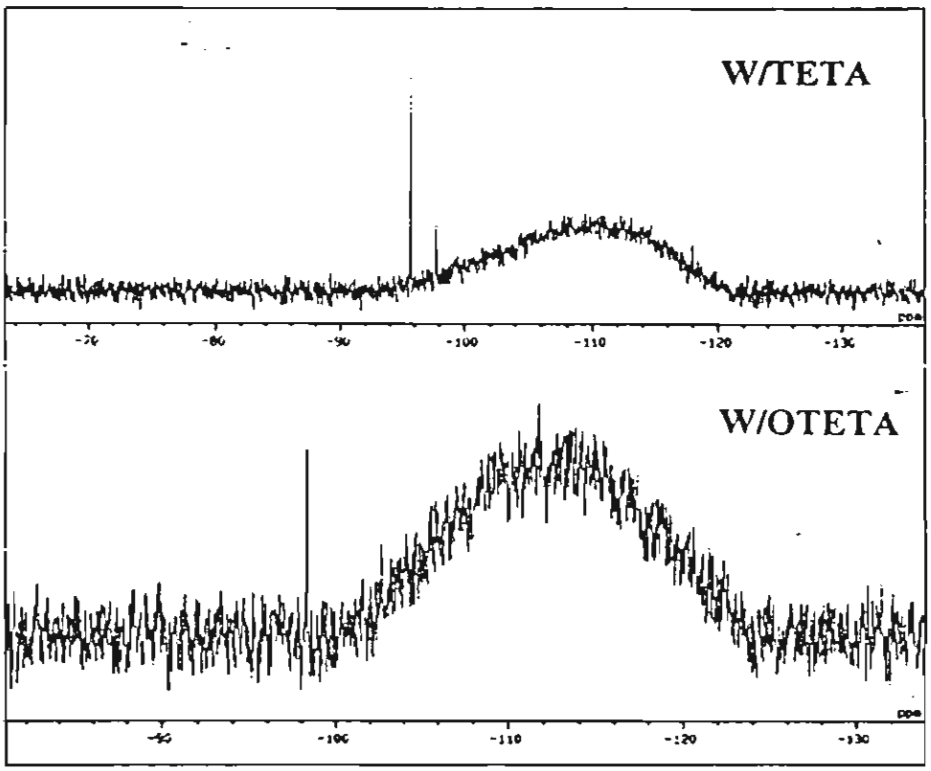

Figure 2.5 : ^{29}Si-NMR Spectra of Silatrane Complexes w/ and w/o TETA

CONCLUSIONS

The silatrane complexes can be synthesized directly from widespread available SiO_2 and TIS via the "Oxide One Pot Synthesis" process in the presence and absence of TETA. When TETA is present, the reaction time is twice faster. Thus, TETA could be used as an accelerator for this reaction. The purified products from the reaction with and without TETA are white solid powder which give molecular ion peaks at m/e=623 and 838, respectively. Other characterization studies show that both products display similar properties.

REFERENCES

1. Kirk-Othmer Encyclopedia of Chemical Technology (1979), 3rd Ed., "Silica", Vol. 20, p. 750
2. R. Tacke and H. Linoh (1989), "Bioorganosilicon Chemistry, in S. Patai and Z. Rappoport", *The Chemistry of Organic Silicon Compounds*, Wiley-Interscience, New York.
3. E. Lukevics and L. Ignatovich (1992), "Comparative Study of the Biological Activity of Organosilicon and Organogermanium Compounds", *Appl.Organomet. Chem.* 6, 113
4. M.G. Voronkov, M.S. Sorokin, V.A. Klyuchnikov, G.N. Shvetz and V.J. Pepekin (1989), "Thermochemistry of Organosilicon Compounds", *J.Organomet.Chem.* 359, 301

5. G. Cerveau, C. Chuit, E. Colomer, R.J.P. Corriu and C. Reye (1990), "Ferrocenyl Compounds Containing Two Hypervalent Silicon Species", *Organometallics* 9, 2415

6. M. Nasim, L.J. Livantsova, P.D. Krutko, G.S. Zaitseva, J. Lorbertth and M. Otto (1991), "Synthesis of 2-Silatranyl-and 2-(3,7,10-trimethylsilatranyl) acetaldehydes", *J.Organomet.Chem.* 402, 313

7. P. Hencsei (1991), "Mass-spectrometric Study of Ring Substituted Silatranes", *Struct.Chem.* 2, 21

8. R.J.P. Corriu and J.C. Young (1989), "Hypervalent Silicon Compounds, in : S. Patai and Z. Rappoport", *The Chemistry of Organic Silicon Compounds*, Wiley-Interscience, New York

9. C. Chuit, R.J.P. Corriu, C. Reye and J.C. Young (1993), "Reactivity of Penta- and Hexacoordinate Silicon Compounds and Their Role as Reaction Intermediates", *Chem.Rev.* 93, 1371

10. V. Gevorgyan, L. Borisova, A. Vjater, J. Popelis, S. Belyakov and E. Lukevics (1994), "Synthesis and Structure of Silylmethylsilatranes RR'R''SICH2SI(OCH2CH2)(3)N", *J.Organomet.Chem.* 482, 73

11. M.G. Voronkov, V.M. Dyakov and S.V. Kirpichenko (1982), "Silatranes", *J.Organomet.Chem.* 233, 1-147

12. M.G. Voronkov (1966), "Silatranes:Intra-Complex Heterocyclic Compounds of Pentacoordinated Silicon", *Pure Appl.Chem.* 13, 35

13. J. Dirk Nies, J.M. Bellama, B-Z. Nava (1985), "Multiphoton Infrared Laser-induced Degradation of Polydimethylsiloxane and Hexamethyldisilane", *J.Organomet.Chem.* 296, 315

14. Rangsitphol, J. (1995), Aryloxysilane Synthesis Directly from silica and Catechol, Master Thesis, The Petroleum and Petrochemical College, Chulalongkorn University.

15. R. Laine, K. Blohowiak, T. Robinson, M. Hoppe, P. Nardi, J. Kampf and J. Uhm (1991), "Synthesis of Pentacoordinate Silicon Complexes from SiO_2", *Nature* 353, 642-644

16. K. Blohowiak, D. Tradewell, R. Mueller, M. Hoppe, S. Jouppi, P. Kansal, K. Chew, C. Scotto, F. Babonneau, J. Kampf and R. Laine (1994), "SiO_2 as a Starting Material for the Synthesis of Pentacoordinate Silicon Complexes", *Chem.Mater.* 6, 2177-2192

17. C. Bickmore and R. Laine (1996), "Synthesis of Oxynitride Powders via Fluidized-Bed Ammonolysis, Part I: Large, Porous, Silica Particles", *J.Am. Ceram.Soc.* 79, 2865-77

18. L. Sommer and O. Bennett (1957), "Anomalous Spin-Spin Splitting in NMR Spectra of Cyclobutenes", *J.Am.Chem.Soc.* 79, 1008

19. J. Turley and F. Boer (1968), "Structural Studies of Pentacoordinated Silicon. I - Phenyl-(2,2',2"-nitrilotriethoxy)silane", *ibid.* 90, 4026

CHAPTER III
SYNTHESIS OF ALUMATRANE

ABSTRACT

Preparations of alumatrane complexes generally are high cost because of multistep synthesis and expensive starting materials. Recently, a new one step method was developed for synthesizing alumatrane directly from aluminum hydroxide [$Al(OH)_3$] and triisopropanolamine (TIS) both of which are inexpensive and readily available. When 45.5 mmol of $Al(OH)_3$ are reacted with 70 mmol of TIS at 200°C, the reaction is complete in 3 h. The product can be purified by precipitation. Triethylenetetramine (TETA), a stronger base than TIS, was found to accelerate the dissolution rate of $Al(OH)_3$. The kinetics of TIS-Al formation were studied and TIS-Al was fully characterized using DSC, TGA, FAB$^+$-MS, NMR (^{1}H-, ^{13}C-, ^{27}Al-), and FTIR. The integral method was used to study the dissolution kinetics as a function of different conditions. The activation energy of reaction was 24±2 kJ mol^{-1}.

INTRODUCTION

Atranes, I, with M = B, Al, Si, Ge, Sn, Pb, P, Ti, V, Mo, etc. have been synthesized and studied during the last three decades[1-5]. These compounds are of interest because of their cage structure, physical/chemical properties, and especially biological activity. The behavior of alumatrane, where M = Al, 2,8,9-trioxa-1-alumatricyclo [3.3.3.0^{1,5}]undecane, and oligomeric alumatrane has been described previously[6-9].)]. In benzene solution, cryoscopy and ebullioscopy indicate tetrahedral and octameric behavior. A mass spectroscopic (EI 70 eV) study showed the stability of the dimer I' in the gas phase.

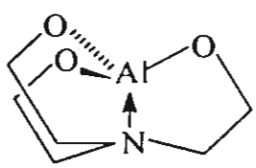

I

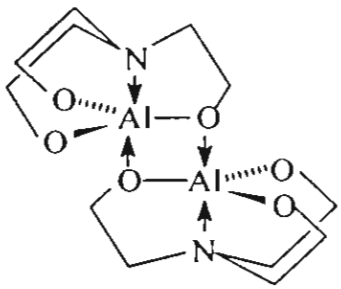

I'

There are several methods of preparing alumatranes. Alumatrane is prepared readily in high yield by reaction of aluminum alkoxides with triethanolamine in an aromatic solvent[10-11] or with no solvent[12-14].

Triethylaluminum also reacts with triethanolamine in toluene or hexane at -78°C to form alumatrane[15]. VERKADE[16] prepared alumatrane by the alcoholysis of tris-(dimethylamido) aluminum with triethanolamine and also the transligation of monomeric and dimeric alumaazatranes with triethanolamine.

According to ^{27}Al-, ^{1}H-, and ^{13}C-NMR data, they found tetramers, II, in solution and dimeric I' by mass spectra in the gas phase. Alumatrane precursors, aluminum alkoxides [$Al(OR)_3$] or aluminum alkyls [$Al(R)_3$], are expensive and the syntheses are multistep. LAINE et al. have developed an inexpensive way to convert metal oxides, namely, alumina and silica, into novel materials ranging from ion conducting, liquid crystalline polymers to oligomeric and polymeric precursors[17-18].

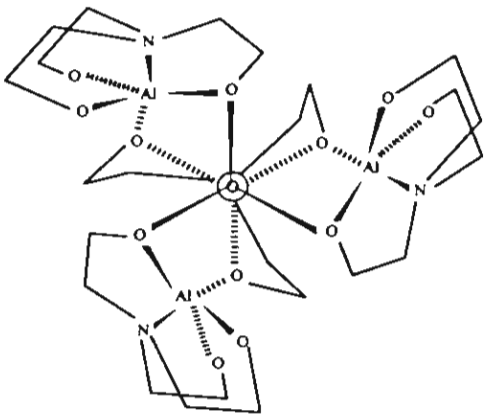

II

LAINE also found that higher boiling point amine bases (b.p.>200°C), such as triethanolamine and triethylenetetramine can be used either in catalytic or stoichiometric quantities to dissolve SiO_2. Moreover, they also found that approximately stoichiometric quantities of TEA will effectively dissolve $Al(OH)_3$. The "Oxide One Pot Synthesis Process (OOPS)" for alkoxyalanes was developed after it was discovered that stoichiometric amounts of TEA would dissolve aluminum hydroxide, the source material for most pure alumina.

The purpose of this work is to extend previous efforts to reactions of aluminum hydroxide ($Al(OH)_3$) and triisopropanolamine (TIS) and study the kinetics of the product formation, which includes the reaction order, rate constant and activation energy. Along with this, the effect of triethylenetetramine (TETA) on the reaction was also studied to improve the solubility of this novel aluminum alkoxide in non-polar solvents for use as a catalytic intermediate in the sol-gel processing.

EXPERIMENTAL

Materials

The starting materials and products are moisture and air sensitive. Therefore, all operations were carried out with careful exclusion of air by purging with nitrogen gas.

UHP grade Nitrogen; 99.99% purity was obtained from Thai Industrial Gases Public Company Limited (TIG). Aluminum hydroxide hydrate [$Al(OH)_3.xH_2O$] containing 57.5% Al_2O_3 content by TGA was purchased from Aldrich Chemical Co. Inc. (USA) and used as received. Ethylene glycol (EG), used as solvent in the reaction, was purchased from Farmitalia Carlo Erba (Barcelona) and purified by fractional distillation at 200°C, under N_2 before use. Triisopropanolamine (TIS) was obtained from Fluka Chemika-BioChemika (Switzerland) and used as received. Triethylene Tetramine (TETA) was obtained from Union Carbide Thailand Limited (Bangkok, Thailand) and distilled under vacuum (10^{-2} torr) at 120°C. Acetonitrile and methanol were purchased from J.T. Baker Inc. (Phillipburg, USA) and purified by standard techniques. Acetonitrile was distilled from calcium hydride powder. Methanol was distilled from magnesium metal activated with iodine.

Instrumentation

Mass spectra were obtained on a 707E-Fison Instrument (VG-Autospec, Manchester, England) with a VG data system, used in the positive fast atomic bombardment (FAB^+) mode. Thermal analysis was carried out on a Netzsch DSC 200 (Germany) and a Netzsch Gerätebue BmbH Thermal analysis TG 209 (Germany). ^1H- and ^{13}C-NMR spectra were obtained using a 500 MHz JEOL (JNM-A500) spectrometer at the Scientific and Instrumental Research Equipment Center, Chulalongkorn University, using deuterated methanol (CD_3OD) and tetramethylsilane (TMS) as the solvent and internal reference, respectively. ^{27}Al-NMR spectra were recorded on Bruker 360 MHz at the University of Michigan. FTIR spectra were recorded on a Bio-Rad FT-45A Fourier transform infrared spectrometer with a resolution of ± 4 cm^{-1}.

Procedure

General procedures to obtain tris(alumatranyloxy-*i*-propyl)amine are as follows; aluminum hydroxide, 50 mL of EG, and TIS were added to a 250 mL two-necked round bottomed flask. The reaction mixture was stirred and heated under N_2 in a thermostatted oil bath. When the oil bath temperature reached 200°C, the reaction was considered to have commenced. Fresh EG in the same amount as the distillate was added to maintain the total reaction volume until the reaction mixture turned clear (about 3 hour), indicating reaction completion. After letting the reaction mixture stand without stirring overnight, white product precipitated out. After filtering, the product was stirred with dried acetonitrile overnight to remove excess TIS. The solid product was then filtered off and dried under high vacuum (10^{-2} torr) at 120°C for 5 h. Dried products were then characterized using DSC, TGA, FTIR, FAB^+-MS and NMR.

Kinetic studies

The kinetic studies were primarily conducted on the dissolution of $Al(OH)_3$ as a function of changes in the reaction conditions, namely, the amount of TIS, the amount of aluminum hydroxide, reaction temperature, and time. Each reaction was repeated three times.

The optimum ratio of TIS was studied by fixing the amount of $Al(OH)_3$ (57.5% Al_2O_3 content by TGA) at 22.7 mmol or 10 mmol equivalent of Al_2O_3. The amount of TIS was varied from 0-50 mmol. The reaction time and temperature were fixed at 3 h and 200°C, respectively.

Dissolution Rate as a Function of $Al(OH)_3$ Concentration

The amount of TIS was fixed at 3.83 g (20 mmol) and the amount of $Al(OH)_3$ was varied from 0.89-8.87 g (5-40 mmol). EG was added to make the total volume of reaction mixture 50 mL. The reaction time and temperature were set at 1 h and 200°C, respectively. Each run was repeated three times. The relationship between mmol of unreacted alumina and mmol of alumina added was plotted.

Dissoluion Rate as a Function of TETA Concentration

To study the effect of [TETA] on the rate of reaction, $Al(OH)_3$ and TIS quantities were fixed at 1.77 g (22.7 mmol) and 0.96 g (5 mmol), respectively. The concentration of TETA was varied from 0-4.3875 g (0-30 mmol). The reaction time and temperature were fixed at 3 h and 200°C. The relationship between mmol dissolved alumina and mmol TETA added was then plotted.

Determination of the Reaction Rate Constant and Activation Energy

Amounts of $Al(OH)_3$ and TIS were fixed at 1.77 g (22.7 mmol) and 0.96 g (5 mmol), respectively. The reaction time was varied from 15-120 min with increments of 15 min at 150°, 170°, 190°, and 200°C. The relationship between mmol of unreacted alumina versus reaction time at each reaction temperature was then plotted to obtain the reaction rate constant (k). The activation energy was then calculated by plotting ln (k) versus 1/T ($1\ K^{-1}$).

Dissolution Rate as a Function of Time in the Presence of TETA as a Catalyst

The effect of time on the reaction of $Al(OH)_3$ and TIS with TETA as a catalyst was studied by fixing the amounts of $Al(OH)_3$, TIS, and TETA at 1.77g (22.7 mmol), 0.96 g (5 mmol), and 0.18 g (1.25 mmol), respectively. The reaction temperature was fixed at 200°C and the reaction time was varied from 15-120 min. The mmoles of unreacted alumina for each run were then plotted versus time.

RESULTS AND DISCUSSION

In this study, recovered $Al(OH)_3$ was thermally converted to α-alumina to determine the actual amount dissolved. $Al(OH)_3$ used at the beginning and left after the reaction was measured as Al_2O_3 using TGA ceramic yield.

As seen in Figure 3.1, with a fixed amount of aluminum hydroxide hydrate [1.77 g (22.7 mmol)] at a reaction time and temperature of 3 h. and 200 °C, respectively, the reaction went very slowly for TIS quantities less than 20 mmol. However, it went to completion when 35 mmol of TIS was used. It was found also that when 10 mmol of TETA was used with the 22.7 mmol of $Al(OH)_3$ and 35 mmol of TIS, the reaction was complete within 2 h.

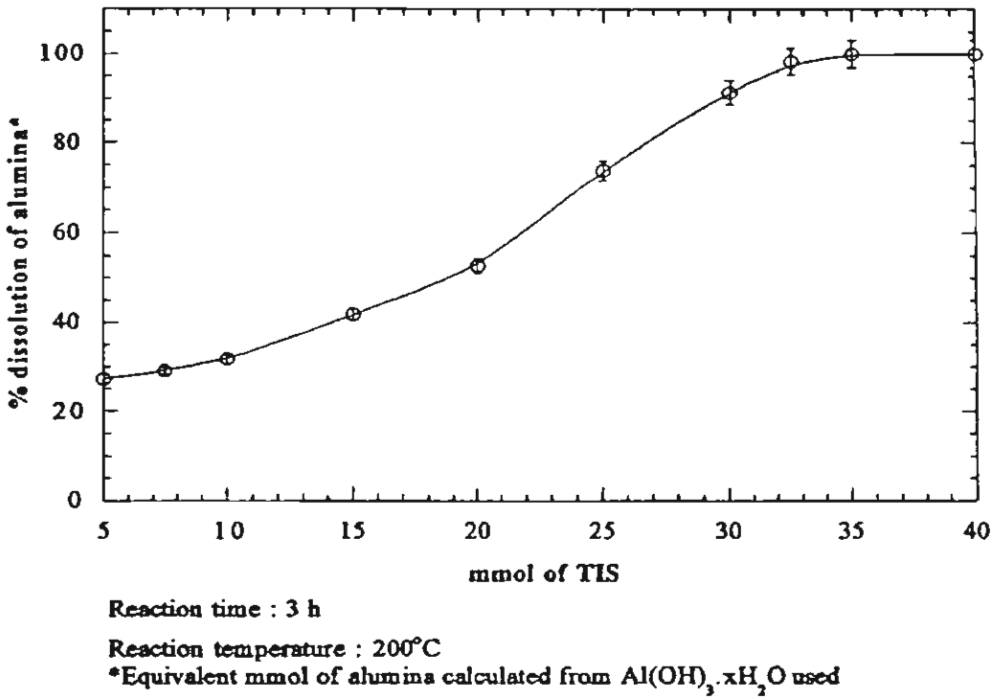

Figure 3.1 Optimization of $Al(OH)_3$:TIS Ratio for Complete Dissolution of $Al(OH)_3$.

Dissolution Rate as a Function of $Al(OH)_3$ Concentration

In this case, determination of a reaction rate, the so-called "method of initial rates", was based upon an accurate analysis of one product at a very early stage of reaction. Therefore, all reactions studied did not proceed to completion. The reaction time and temperature were thus set at 1 h and 200°C. The amount of alumina was varied from 7.5 to 12.5, 15, and 40 mmol while the concentration of TIS was fixed at 20 mmol. The relationship between the dissolved and added alumina is nearly linear, as shown in Figure 3.2. Clearly, the reaction of $Al(OH)_3$ and TIS also depended on the concentration of $Al(OH)_3$. The curve was nearly linear, suggesting that the reaction was first order with respect to $Al(OH)_3$ and first order with respect to TIS. It is worth noticing that the intercept of both curves are not equal to zero. This is because some unreacted $Al(OH)_3$ was lost during recovery step.

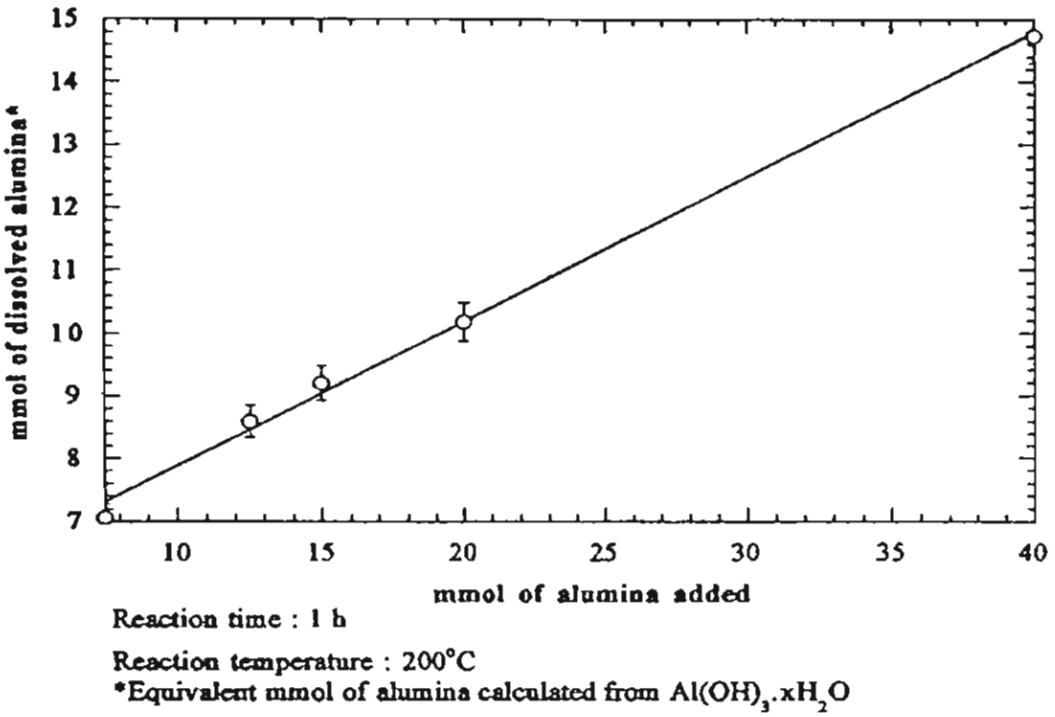

Figure 3.2 Dissolution Rate as a Function of $Al(OH)_3$ Concentration.

Determination of the Reaction Rate Constant and the activation energy

We used the integral method to determine the reaction order. The reaction order was assumed to be second order overall. Plots of ln[(1-rX)/(1-X)] versus reaction time at each temperature are presented in Figure 3.3, (Note:the linearity of the data suggesting that the reaction is most likely to be second order as assumed). The reaction rate constants were obtained from the slope of the plotted data, straight line with different gradients. As expected, the higher temperature showed the higher gradient, meaning that the higher reaction temperature, the higher dissolution rate.

To determine the activation energy, the Arrhenius equation was employed. From section 3.2.3, after obtaining the reaction rate constants (k), ln k was plotted versus 1/T(1/Kelvin) as Figure 3.4, which gives a straight line with the slope proportional to the activation energy. The slope obtained is equal to the activation energy devided by the gas constant (8.314 J mol^{-1} K^{-1}). As a result, the activation energy was 24 ± 2 KJ mol^{-1}.

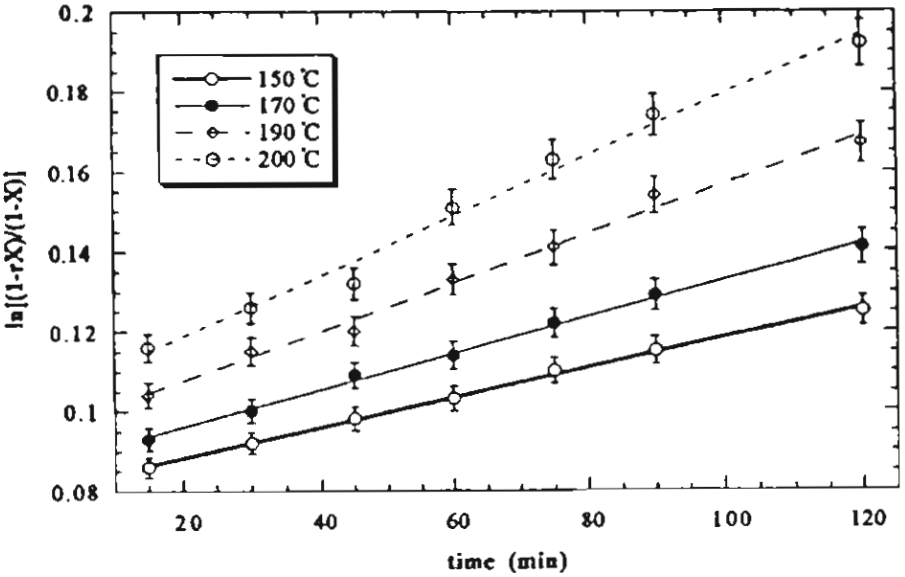

Figure 3.3 The Relationship of Logarithm of Conversion Factor versus Reaction Time for each Variation of Reaction Temperature.

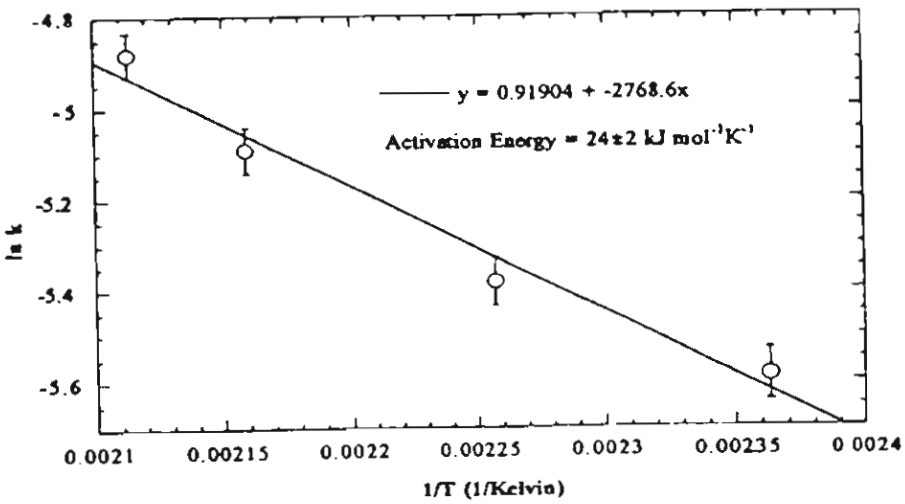

Figure 3.4 The Relationship of Logarithm of Rate Constant and Reaction Temperature.

Dissolution Rate as a Function of TETA Concentration

The plot of the amount of dissoved $Al(OH)_3$ and amount of TETA is presented in Figure 3.5. The higher the TETA concentration, the greater the amount of dissolved $Al(OH)_3$. At low TETA concentration (1.25-2.5 mmol), the amount of $Al(OH)_3$ dissolved increased significantly, as compared to the higher TETA

concentrations. This is due to the role of TETA acting as solubilization catalyst to increase the surface area of $Al(OH)_3$.

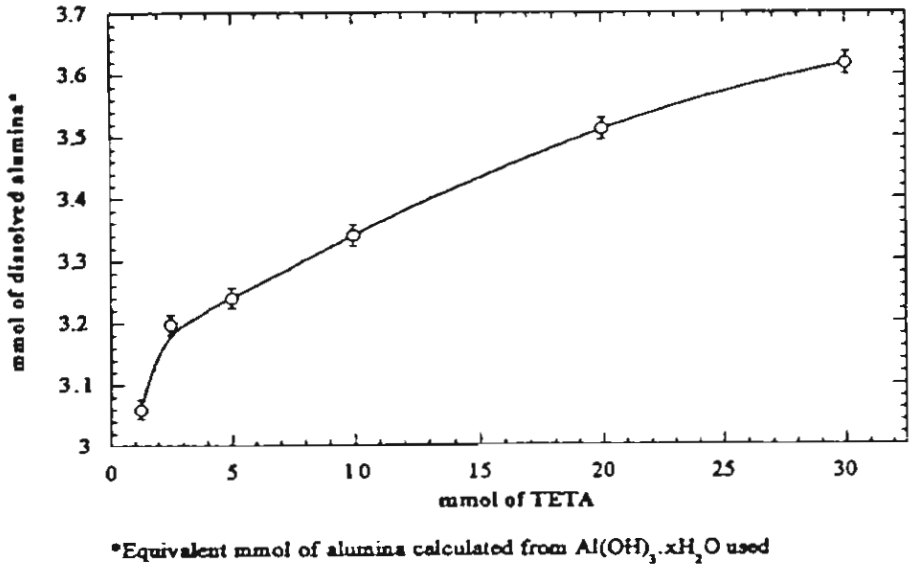

Figure 3.5 Effect of the TETA Concentration.

Dissolution Rate as a Function of Time in the Presence of TETA as a Catalyst

Figure 3.6 shows a plot of mmol of unreacted $Al(OH)_3$ versus reaction time comparing reactions with (1.25 mmol) and without TETA. The dissolution reaction rate with TETA was faster than that without TETA because TETA increased solubility of $Al(OH)_3$, resulting in increasing its surface area which caused the reaction to go faster, as discussed previously.

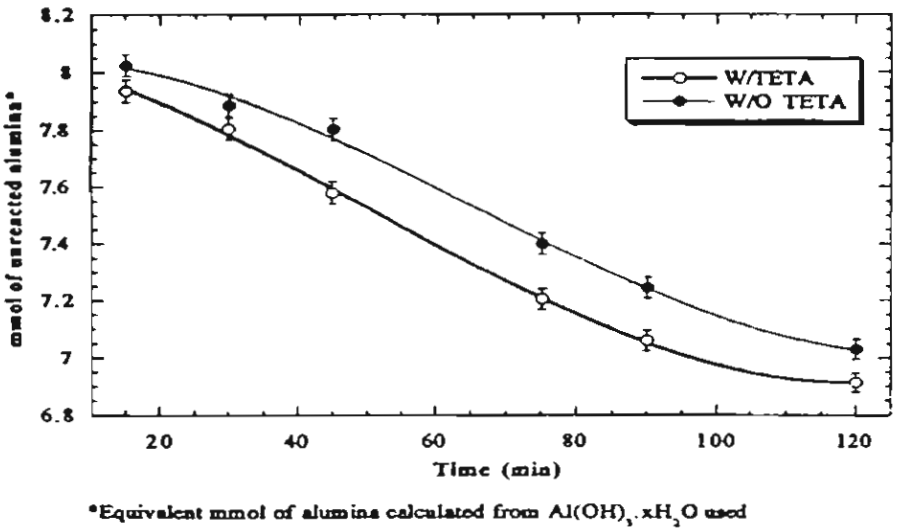

Figure 3.6 Effect of TETA Concentration with Time.

Characterization

Thermogravimetric Analysis

The TGA data for the product from the reaction without TETA (Figure 3.7 (a)) shows two major regions of mass loss. The first region was between 180°-260°C that indicated the decomposition of TIS which is a component of the product while the second region occurred at about 260°-550°C which corresponded to the oxidative decomposition of the organic ligands and carbon residues. The % ceramic yield of the product was 27.6 %, which was higher than the theoretical ceramic yield (23.7 %) owing to the incomplete combustion of the sample since the final ash was still gray in color.

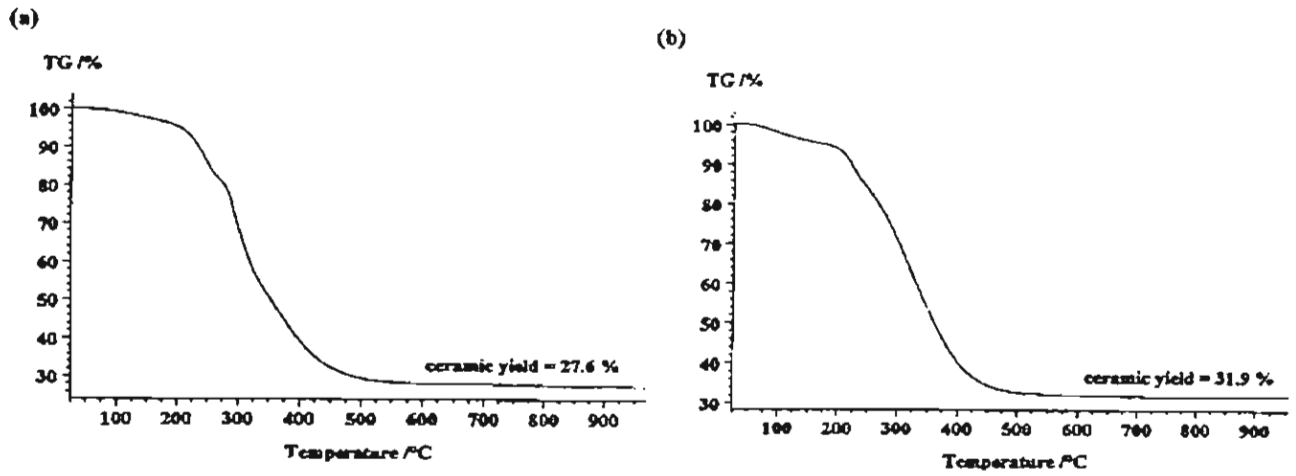

Figure 3.7 TGA Thermogram of the Product from the Reactions: (a) with and (b) without TETA.

Similarly, the TGA of the product synthesized in the presence of TETA (Figure 3.7(b)) also showed two major mass losses at 180°-250°C and 250°-500°C corresponding to the decomposition of TIS ligand and the oxidative decomposition of the organic ligands, and carbon residues, respectively. The % ceramic yield of product was 31.9 %, which was much higher than the theoretical yield. This can be explained along with the mass spectrum which indicated that the product synthesized from the batch with TETA gave more dimer (m/e 431) than the one without TETA because mass spectral data showed that the product consists of monomer, trimer, pentamer, and hexamer. The more smalller unit, the higher ceramic yield. Moreover, the final ash was darker in color.

Differential Scanning Calorimetry

The DSC of the product from the reaction without TETA (Figure 3.8(a)) showed an exotherm at 250°-280°C corresponding to the boiling point of TIS, since when the product was run the second time, there was no exothermic peak in DSC thermogram. An endotherm at 380°-400°C, as

compared to its TGA, correlated to the decomposition temperature of products. The T_g was observed at about 167°C.

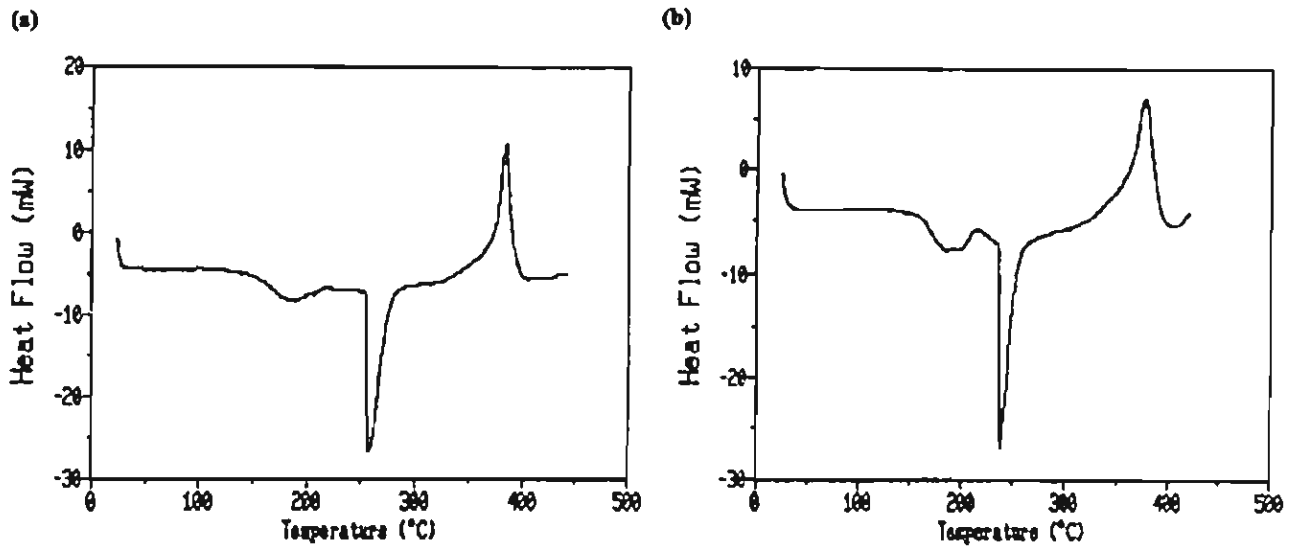

Figure 3.8 DSC Thermograms of the Product from the Reactons (a) with and (b) without TETA.

Similarly, the DSC data of the product from the reaction with TETA (Figure 3.12) showed the exotherm at about 220°-260°C corresponding to the decomposition of TIS. An endotherm at about 350°-400°C was again the decomposition temperature of products. The T_g of this product occured at about 166°C

FAB$^+$*-Mass Spectroscopy*

Mass spectral analysis suggests that there are four different alumatrane complexes; hexamer (m/e 1292), the highest intensity pentamer plus one morpholine (m/e 1250), resulted from losing a molecule of water in TIS, trimer plus one ethylene glycol (m/e 707), and monomer plus one TIS (m/e 409) and the intensities of all proposed structures was shown in table 3.1.

The fragmentation pattern of the product from the reaction with TETA gave higher intensities of the lower unit peaks at m/e 216 and 409, and lower intensity of the peak at m/e 1250. This result can obviously confirm that the reaction carried out without TETA gives the product containing higher molecular weight unit than the one run with TETA owing to the acceleration of TETA resulting in faster completion of the reaction.

Table 3.1 The Proposed Structures and Fragmentation Pattern of Products

m/e	Intensities	Proposed Structure
216	50	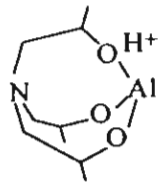 $AlN(CH_2CH_2CH_3O)_3H^+$
409	17.5	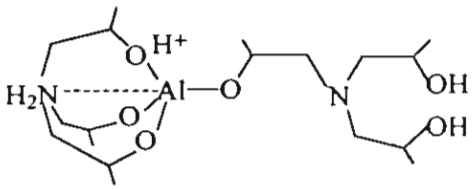 $AlN(CH_2CH_2CH_3O)_3N(CH_2CH_2CH_3O)\ (CH_2CH_2CH_3OH)_2H^+$
492	38.7	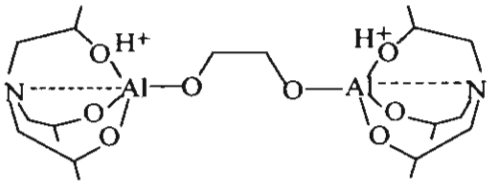 $Al_2[N(CH_2CH_2CH_3O)_3]_2\ (OCH_2\ CH_2O)\ H_2^+$
707	35.4	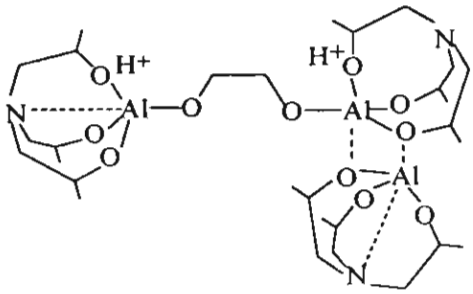 $Al_3[N(CH_2CH_2CH_3O)_3]_2(OCH_2)_2H_2^+$
959	7.9	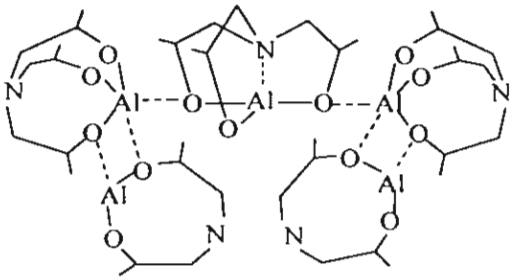 $Al_3[N(CH_2CH_2CH_3O)_3]_2Al_2[N(CH_2CH_2CH_3O)_2]_2$

1076	15	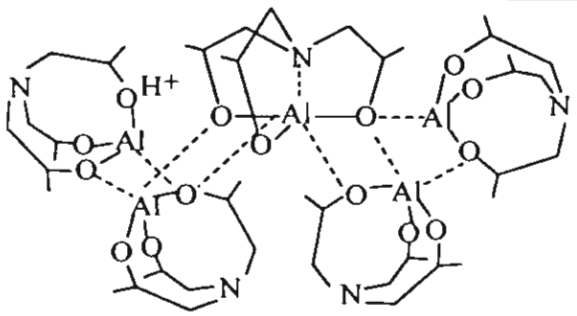 $Al_5[N(CH_2CH_2CH_3O)_3]_5H^+$
1175	46.3	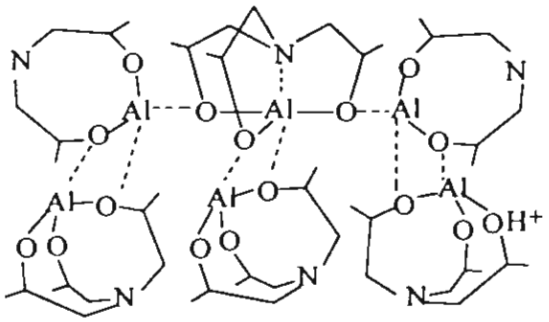 $Al_4(CH_2CH_2CH_3O)_3]_4Al_2[N(CH_2CH_2CH_3O)_2]_2H^+$
1250	100	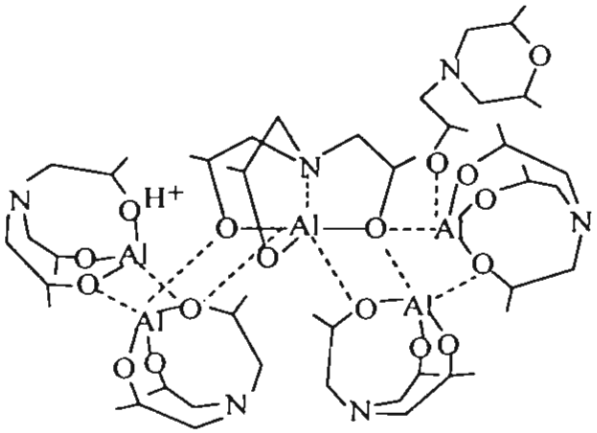 $Al_5[N(CH_2CH_2CH_3O)_3]_5N(CH_2CH_2CH_3O)_2CH_2CH_2CH_3H^+$
1292	7.8	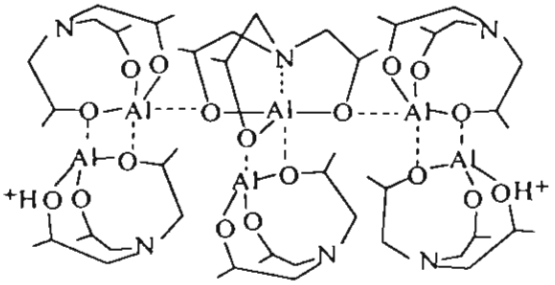 $Al_6[N(CH_2CH_2CH_3O)_3]_6H^+$

Nuclear Magnetic Resonance Spectroscopy

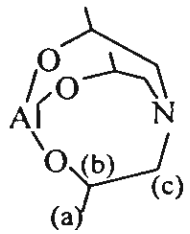

The NMR results showed that the products certainly contained several kinds of oligomers, such as monomer, dimer, etc., which are coincided with the mass spectroscopy results. The ^{1}H-NMR spectrum of the product from the reaction without TETA showed 3 multiple characteristics of quadrapolar coupling peaks indicating the presence of a few species in the product. The peaks at 1.1-1.4 ppm correspond to the -CH_3 group of TIS (position (a)). The peaks at 2.4-3.1 ppm are assigned to the methylene group adjacent to the N-atom of TIS (-N-CH_2) at position (c). The peaks at 3.6-4.2 ppm are assigned to the tertiary carbon adjacent to the O-atom of TIS, position (b). The ^{1}H-NMR spectrum of the product from the reaction with TETA gave a similar one.

Similarly, the ^{13}C-NMR spectrum of the product from the reaction without TETA showed a multiple peak at 22.0 ppm corresponding to -CH_3 groups at position (a) coupled to itself and proton of the tertiary carbon. The sharp peak at 64.3 ppm belongs to the carbon adjacent to N-atom of TIS (-N-CH_2) at position (c). The multiple peak at 79.0 ppm is associated with the carbon adjacent to O-atom of TIS (position (b)) due to the coupling with -N-C$\underline{H}_2$ and -C$\underline{H}_3$. The spectrum of both reactions showed the similar positions.

The ^{27}Al-NMR spectra of the products from the reaction with and without TETA coincidentally showed 3 multiple peaks, as shown in Table 3.2, at around 65, 49 and 7 ppm at the ratio of 1:1:1. Again, these three peaks indicated the presence of both hexa- (at 7 ppm) and tetracoordinated (at 65 and 49 ppm) aluminum compounds.

Fourier Transform Infrared Spectroscopy

The FTIR spectra of the products from the reactions with and without TETA show similar functional groups (Table 3.3). Due to the moisture sensitivity of the products, the ν O-H appears at 3300-3700 cm^{-1}, and the wave number at 2750-3000 cm^{-1} corresponds to ν C-H. The single peak at about 1650 cm^{-1} is O-H overtone and C-H bending. The strong peak at 1000-1250 cm^{-1} results from the ν C-N and/or O-H bending. The broad peak at 500-800 cm^{-1} represents the ν Al-O of the product.

Table 3.2 Peak Positions of ^{1}H- , ^{13}C-, and ^{27}Al-NMR of Products

Compounds	^{1}H-NMR (ppm)	^{13}C-NMR (ppm)	^{27}Al-NMR (ppm)
Product w/o TETA	1.07-1.41 (a) 2.36-3.15 (c) 3.65-4.23 (b)	21.59-22.45 (a) 64.30 (c) 78.56-79.21	7.5 49.6 66.0
Product w/ TETA	1.07-1.88 (a) 2.23-2.85 (c) 3.73-4.11 (b)	20.79 (a) 64.30-65.63 (c) 78.79-79.48 (b)	7.4 48.8 64.9

Table 3.3 Peak Position and Assignments of FTIR Spectra of Products with/without TETA

peak positions		assignments
Al-TIS	TIS-Al-TETA	
3000-3700	3000-3700	u O-H and u C-H
2750-3000	2750-3000	u C-H
1650	1630	O-H overtone; C-H bending
1450	1450	δ C-H
1000-1200	1000-1250	u C-N; O-H bending
500-800	500-800	u Al-O

CONCLUSIONS

In this work, alumatrane complexes were synthesized directly from inexpensive starting material, aluminum hydroxide, and TIS, via the one step process, called "OOPS" process. Mass spectra revealed that products were oligomers. The main product was pentamer bonded with TIS that lost one H_2O molecule. From TGA data, the % ceramic yields of the product from the reactions without and with TETA were 27.6 and 31.9 %, respectively, which are higher value than the theoretical yield (23.7%). The higher percent ceramic yields were due to the small unit of oligomers in the product and the small amount of unreacted $Al(OH)_3$ remaining in the product.

The reaction order was second order overall, first order with respect to aluminum hydroxide and first order with respect to TIS. The dissolution rate increased when the reaction temperature increased. The activation energy of this reaction was about 24 ± 2 KJ mol^{-1}.

REFERENCES

1. Voronkov, M. G., Seltschan, G. I., Lapsina, A. and Pestunovitsch, V. A., *Z. Chem.*, 1968, 8.
2. Voronkov, M. G., *Vestnik Akad. Nauk SSSR*, 1968, 38, 48
3. Voronkov, M. G. and Zelchan, G. I., *Khim. geterotsikl. soed.*, 1965, 51.
4. Bradley, D. C., Mehrotra, R. C., Gaur, D. P., *Metal Alkoxides;* Academic Press: N. Y., 1978, 266.
5. Pinkas J., Verkade G., *Inorg. Chem.*, 1993:32:2711.
6. Hein, F. and Albert, P. W. Z., *Anorg. Allg. Chem.*, 1952, 269, 67.
7. Mehrontra, R. C. and Mehrotra, R. K., *J. Indian Chem. Soc.*, 1962, 39, 677.
8. Mehrotra and Rai, A. K., *Polyhedron*, 1991, 10, 1967.
9. Shklover, V. E., Struchkov, Yu. T., Voronkov, M. G., Ovchinnikova, Z. A. and Baryshok, V. P., *Dokl. Akas. Nauk (Engl. Transl)*, 1984, 227, 723.
10. Voronkov, M.G., Baryshok, V.P., *Organomet. Chem.*, 1982:239:199.
11. Thomas, W. M., Groszos, S. J and Day, N. E., *U.S. Patent 2*, 1961, 985, 685; *Chem. Abstr.*, 1961, 55, 20966.
12. Icken, J. M. and Jahren, E. J., *Belg. Patent 619*, 1963, 940; *Chem. Abstr.*, 1963, 60, 2768.
13. Stanley, R. H., *British Patent 1*, 1968, 123,559; *Chem. Abstr.*, 1968, 69, 78532.
14. Elbing, I. N. and Finestone, A. B., *German offen 1.*, 1964, 1,162,439; *Chem. Abstr.*, 1964, 60, 17/4705.
15. Higashi, H. and Namikawa, S., *Kogyo Kagaku Zasshi*, 1967, 70,97.
16. Verkade, J. K., *Acc. Chem. Res.*, 1993, 26, 483.
17. Blohowiak, K., Tradewell, D., Mueller, R., Hoppe, M., Jouppi, S., Kansal, P., Chew, K.W., Scotto, C., Babonneau, F., Kampf, J. and Laine, R.M., *Chem. Mater.*, 1994:6:2177-92
18. Ray, D. G., Laine, R. M., Robinson, T. R., Viney, C., *Mol. Crys. Liq. Crystal*, 1992, 225,153.
19. Laobuthee, A., Wongkasemjit, S., Traversa, E. and Laine, R., *J. Eur. Cer. Soc.*,2000, 20,185-191.

CHAPTER IV
SOL-GEL PROCESSING OF SILATRANES

ABSTRACT

Silatrane complexes are organosilicon compounds synthesized by direct reaction of SiO_2 and trialkanolamines. Here, we explore their potential as ceramic precursors via the hydrolytic sol-gel processing method. Viscoelastic analysis is used to characterize the gelation behavior of silatranes based on triisopropanolamine, under different hydrolysis conditions. Pyrolysed ceramic products are characterized in terms of surface area and morphology and found to have a homogeneous microporous structure with high surface areas (313-417 m^2/g). Faster hydrolysis rates lead to shorter gelation times, and smaller pore sizes in the derived ceramic.

INTRODUCTION

Organosilicate polymers are of interest for their potential as precursors in sol-gel processing to form complex preceramic shapes and structures, not readily accessible by melt processing[1-2]. Due to widespread availability and low cost, silica, (SiO_2) is the ideal starting material to make organosilicon polymers. However, the Si-O bond is very strong and difficult to manipulate chemically[3]. As a corollary, organosilicate polymers, once formed, are very easy to hydrolyze back to SiO_2. Such high reactivity can create problems in chemical processing, therefore it is advantageous to be able to create precursors with reduced hydrolytic activity.

Silatrane complexes are a family of organosilicate compounds derived from reaction of SiO_2 with trialkanolamines such as triethanolamine or triisopropanolamine[4-6]. These materials are hydrolytically stable in air for periods up to several weeks. For this reason, they are candidates for use as precursors in ceramic processing via the sol-gel technique. Here, we report some preliminary viscoelastic studies of sol-gel processing of silatranes under different hydrolysis conditions, and investigate the characteristics of glasses formed by pyrolysis of the products.

EXPERIMENTAL

Synthesis of Silatrane Complex

Materials

Fumed silica (surface area 280 m^2/g, average particle size of 0.007 μm) was purchased from Aldrich Chemical Company, and dried in an oven at 90 °C for 10 hr. Ethylene glycol, purchased from Labscan, was used as reaction solvent, and purified by fractional distillation at 200 °C under N_2 atmosphere. Triisopropanolamine [TIS, $N(CH_2CHCH_3OH)_3$] was obtained from Fluka Chemical Company, and dried in a desiccator. Commercial grade triethylenetetramine [TETA,

$H_2NCH_2(CH_2NHCH_2)_2\ CH_2NH_2]$, supplied by Union Carbide Thailand, Limited, was purified by vacuum distillation at 120 °C (1mm Hg).

Anhydrous diethyl ether and dichloromethane, used as precipitants, were purchased from Baker Analytical Co. Dichloromethane was distilled over anhydrous calcium chloride under N_2 atmosphere. Anhydrous diethyl ether was dried by adding anhydrous calcium chloride, let stand for 24 hr with occasional shaking, and then filtered into a clean dry bottle. HPLC grade tetrahydrofuran, used as solvent for molecular weight determination by gel permeation chromatography, was purchased from J. T. Baker Inc., and used as received.

Reaction conditions

As discovered by Piboonchaisit[6], silatrane complexes were formed by mixing fumed silica with TIS (and TETA as catalyst) in ethylene glycol (EG) as solvent. The reaction temperature was set at the distillation point of EG (200 °C). Water formed during the reaction, and EG were continuously removed and replaced by an equivalent amount of fresh EG distillate. After reaction, the residual EG was removed by vacuum distillation (1 mm Hg). Based on GPC analysis described below, four distinct chemical species may be formed during the reaction, with proposed structures shown in Fig. 4.1, whose relative abundance depends on the molar ratio of TIS:SiO_2, the amount of TETA catalyst present, the temperature at which the vacuum distillation of EG is carried out, and on the duration of this distillation procedure. Of the four structures shown, that with molecular weight 407 is particularly undesirable, because the silicon content is low, and hence the % ceramic yield is poor, which makes the product unsuitable as a ceramic precursor. The optimal reaction condition, at which minimal formation of this species occurs, was found to be at a 1: 1 molar ratio of TIS:SiO_2, (with TETA in the amount of 5 mol% of silica[6]). As the vacuum distillation temperature increases, the amount of high molecular weight species increases up to 180 °C, after which it decreases again, as shown in Fig. 4.2. The optimum temperature for high ceramic yield is therefore 180 °C.

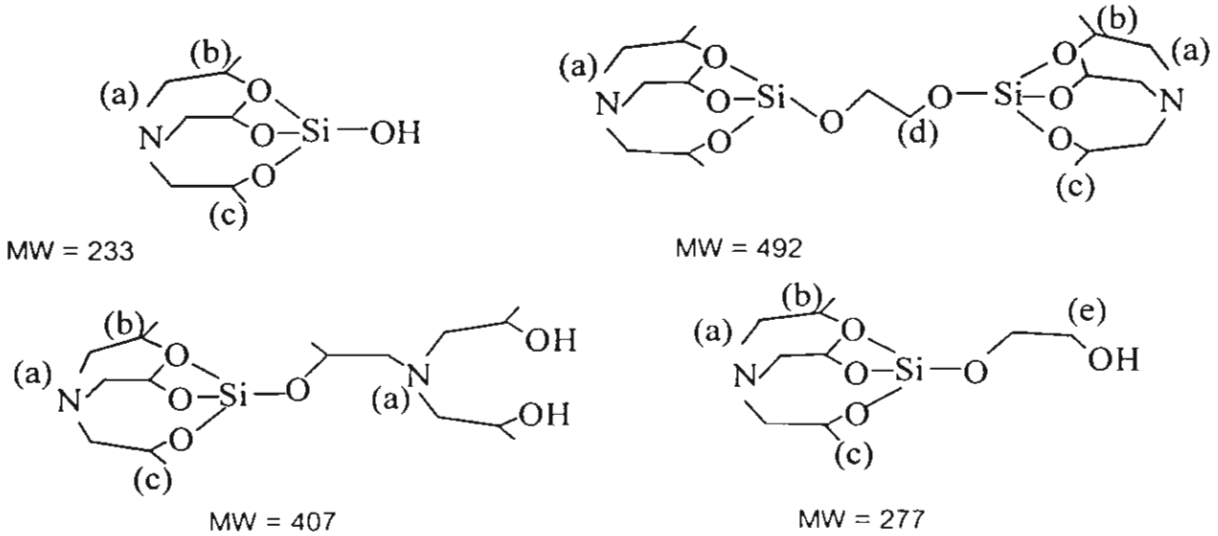

Figure 4.1 The proposed structures of silatrane complexes using 1:1 ratio of [TIS]: [SiO_2].

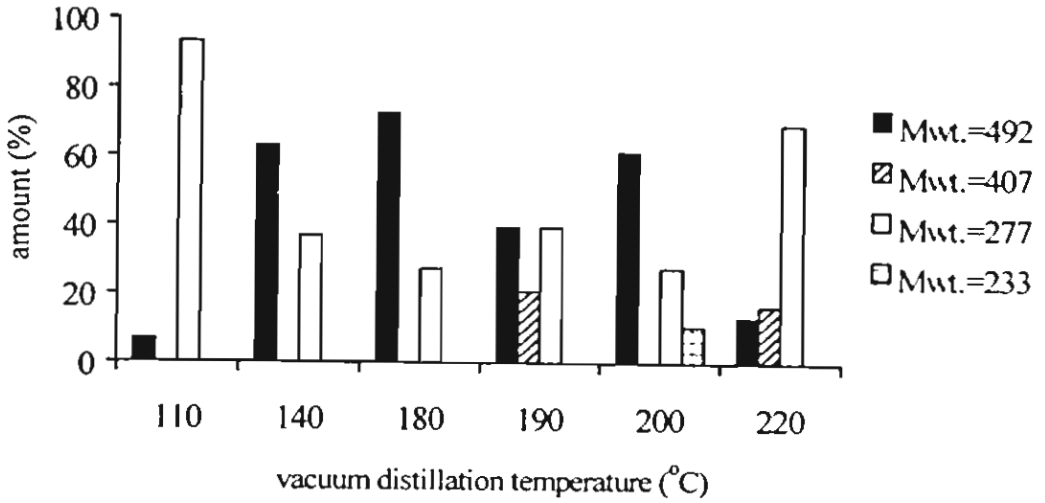

Figure 4.2 Silatrane complexes obtained at 1:1 [TIS]:[SiO_2] and various vacuum distillation temperature.

Characterisation of Silatrane Complexes

FTIR Spectroscopy

FTIR spectroscopic analysis was performed using a Bruker instrument with a resolution of 4 cm^{-1}. Powdered specimens containing 1.0% sample mixed with 99% crystalline KBr were compressed into pellets. The pellets were placed in the sample chamber purged with N_2 for 20 minutes to remove CO_2.

NMR Spectroscopy

^{13}C and ^{1}H NMR spectra of silatrane complexes were obtained using a 500MHz JEOL spectrometer. Samples were dissolved in deuterated DMSO. Tetramethylsilane was used as the internal reference for both proton and carbon NMR.

Gel Permeation Chromatography

GPC chromatograms were performed using a Waters 600E Instrument equipped with UV and RI detectors (Waters 486 and 410, respectively). The column used was Styragel of pore size suitable to separate molecular weights in the range 0 to 1,000. Calibration was performed using polystyrene standards of narrow molecular weight distribution. THF was the solvent at ambient temperature. The silatrane samples were dissolved in THF at concentration below 0.3% weight, and filtered through 0.45 μm membrane filters prior to GPC analysis.

Rheological determination of the sol-gel transition

The transformation from a sol to a gel can be monitored rheologically by following the change in viscoelastic properties. The silatrane reaction product, after removal of residual ethylene glycol, has the appearance of a hard plastic, and was used without further purification. The material was dissolved in the hydrolysis solvent at a concentration of 150% w/v. The hydrolysis temperature was selected to be 40 °C, 50 °C, or 60 °C. The solution was stirred until homogeneous and preheated in a water bath at

the hydrolysis temperature, until the solution was viscous enough to be transferred to the rheometer. The cone and plate attachment of the rheometer was pre-heated to the hydrolysis temperature. The gelation time was determined from the point during pre-heating at which the solution reached the hydrolysis temperature in the water bath. Measurements of storage ($G'(\omega)$) and loss ($G''(\omega)$) moduli were made in a Rheometrics ARES rheometer with a 10g-cm transducer, in cone and plate geometry (cone radius 50 mm, cone angle 0.04 radians). Measurement of $G'(\omega)$ and $G''(\omega)$ was performed at 10 frequencies ω ranging from 0.1 to 1.6 rad/sec. Each frequency scan required 10 sec.

The precise location of the gel point as determined from viscoelastic measurements has been discussed in the previous literature[7]. Initially, the material in the sol state is a viscous fluid such that $\tan\delta = G''(\omega)/G'(\omega) >> 1$. As gelation proceeds, G' and G" increase and, ultimately, the material becomes an elastic gel, $\tan\delta << 1$. Frequently, it is assumed that the gel point occurs at the location of the crossover of the loss (G") and storage (G') moduli (i.e. where $\tan\delta = 1$). However, experimentally, this crossover point is often found to depend on the deformation frequency, ω. A more definitive analysis is now possible following more recent experimental and theoretical work[7-8]. At the gel point, power-law behavior is observed in the frequency dependence of dynamic mechanical experiments. Specifically, the storage and loss moduli follow the relationships[7-8]:

$$G'(\omega) = G''(\omega)/\tan(n\pi/2) = \Gamma(1-n)\cos(n\pi/2)S\omega^n \qquad (4.1)$$

where $\Gamma(1-n)$ refers to the gamma function of argument (1-n). The phase angle δ between stress and strain is independent of frequency and proportional to the relaxation exponent, n:

$$\delta = n\pi/2 \qquad (4.2)$$

A variety of experimental studies have been reported[7, 9-12], which support the validity of this viscoelastic definition of the gel point, including both chemically and physically cross-linked systems. Experimental values of the relaxation exponent n vary from $n \cong 0.2$ to $n \cong 0.8$. For certain chemically cross-linked systems, n depends on stoichiometry. Theoretical predictions, which support various values of the dynamical exponent, n, have been reported[7, 13-14]. Physically, the power law dependence of the moduli originates in the fact that the gel point occurs when the first sample-spanning gel cluster forms. Hence, the magnitude of the dynamical exponent is determined by the structure and hydrodynamic properties of the critical cluster. The power-law behavior originates in the fact that the structure of the critical gel has a fractal character[14].

Characterisation of Pyrolysis Products

BET Surface Area Measurement

The surface area of pyrolysed polysilatrane gels was determined using an Autosorb-1 Gas Sorption System (Quantachrome Corporation) via the Brunauer-Emmett-Teller (BET) method. A

gaseous mixture of nitrogen and helium was allowed to flow through the analyser at a constant rate of 30 cc/min. Nitrogen was used to calibrate the analyser, and was also used as the adsorbate at liquid nitrogen temperature. Each sample was degassed at 300 °C for 2 hr before analysis. The surface area was obtained from a five-point isotherm at P/P_o ratio less than 0.3. The results were computed based on the desorption surface area and the dried weight of the sample after analysis.

Scanning Electron Microscopy

SEM micrographs were obtained using a JEOL 5200-2AE(MP 15152001) scanning electron microscope. Samples were prepared for SEM analysis by attachment to Aluminum stubs, after pyrolysis at 800 °C. Prior to analysis, the specimens were dried in a vacuum oven at 70 °C for 5 hr, and then coated with gold by vapor deposition. Micrographs of the pyrolysed sample surfaces were obtained at 2,000 and 7,500 magnification.

RESULTS AND DISCUSSION

Structural Characterisation of Silatrane Complex

Silatrane complexes produced by the synthetic method described above are a mixture of four molecular species, based on GPC analysis. Proposed structures of each species are shown in Fig. 4.1. Evidence for the formation of silatrane complexes includes observation of characteristic absorption bands in FTIR analysis (Table 4.1) and resonance frequencies in ^{13}C and ^{1}H NMR spectroscopy (Table 4.2).

Table 4.1 Assignments of infrared spectra of the products.

Characterization	Silatrane Complexes
Si-N stretching[a]	560-590 cm^{-1}
Si-O-CH[b]	970,883 cm^{-1}
C-O[a]	1013-1070 cm^{-1}
$Si-O-CH_2$[b]	1015-1085 cm^{-1}
C-N[a]	1270 cm^{-1}
C-H bending[a]	1380-1460 cm^{-1}
C-H stretching[a]	2800-29760 cm^{-1}

a: Silverstein *et al.* 1991.

b: Anderson D.R., 1974.

Table 4.2 ^{1}H-and ^{13}C-NMR chemical shifts of silatrane complexes

Position	Groups	^{1}H-NMR (ppm)	^{13}C-NMR (ppm)
(a)	N-C<u>H</u>$_2$	2.86-2.91	57.7
(b)	CH-C<u>H</u>$_3$	4.0	23
(c)	C<u>H</u>-CH$_3$	0.96-1.12	20-21
(d)	C<u>H</u>$_2$-O	3.3	59.2
(e)	C<u>H</u>$_2$-OH	3.4-3.5	62.5-65

Rheological analysis of Sol-Gel transition of Silatranes

Silatrane complex formed after vacuum distillation of ethylene glycol was dissolved in one of three hydrolysis solvents at a concentration of 150 % w/v. The hydrolysis solvents were: distilled de-ionized water with measured pH = 6.7; MgO solution prepared by dissolving 0.5 g MgO in 1 liter distilled de-ionized water with measured pH = 11.3; and a solution of methanol in distilled de-ionized water at a ratio 1:1 (pH = 8.1). The change in G' and G" was observed following procedures described above. In Fig. 4.3, we show frequency scans of G' and G" during hydrolysis in water at 40 °C at three times, viz. before the gel point, at the gel point, and after the gel point. The location of the gel point was identified following the discussion of Chambon and Winter[7], summarized above in equations (4.1) and (4.2), as the point where G' and G" follow the same power law with exponent n, i.e. a frequency-independent tanδ. As evident in Fig. 4, this occurs at gel time t = 15600 s $\pm$ 1100 s, when n ~ 1.0 and tan δ ~ 1.0. The corresponding variation of tanδ, the apparent frequency exponents of G' and G", and the change in magnitude of the dynamic viscosity, $\eta^*(\omega)$, during hydrolysis are shown in Figs. 4.4, 4.5, and 4.6, respectively. As evident in Figs. 4.4 and 4.5, there is considerable uncertainty (~$\pm$ 7%) in deciding the location of the gel point based on the frequency-independence of tanδ, and, therefore, a corresponding uncertainty in the precise values of the dynamic exponent n = 0.55 $\pm$ 0.15. Fig. 4.6 confirms that, as expected, the dynamic viscosity increases dramatically at the gel point and, after gelation, exhibits a strong dependence on deformation frequency.

Hydrolysis experiments were carried out at three temperatures, and the gel times determined are tabulated in Table 4.3. At each temperature, as illustrated by Roy and McCarthy[15-16], the shortest gel times are observed in the most ionic MgO solvent, where the hydrolysis rate is fastest, and the longest gel times are in the least ionic MeOH solvent, which has the slowest hydrolysis rate. Also increase of temperature increases the rate of hydrolysis and thus decreases the gel times.

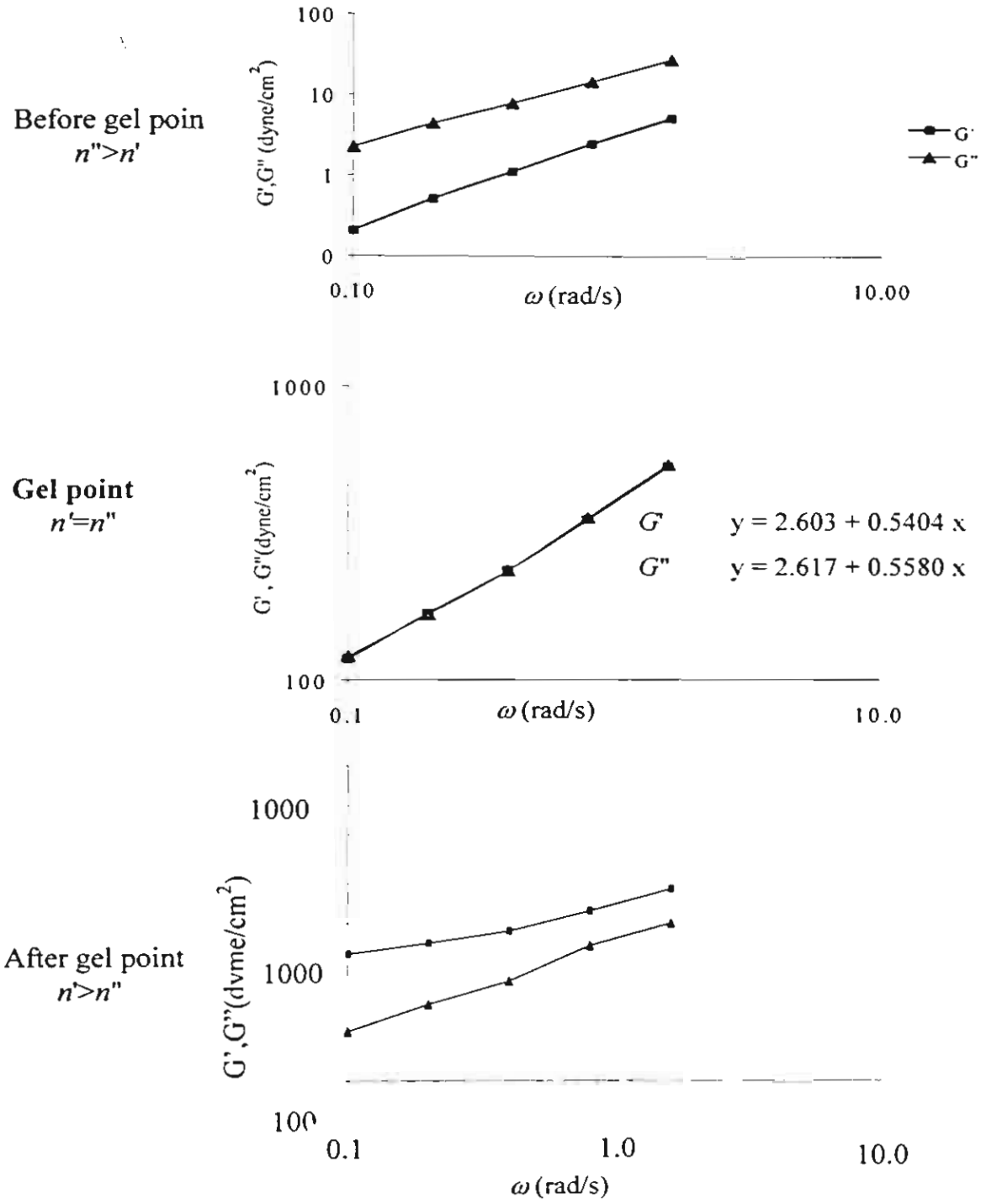

Figure 4.3 The relationship of log G' and log $G"$ vs. log frequency of 150% w/v silatrane complex hydrolyzed in water at T = 40°C.

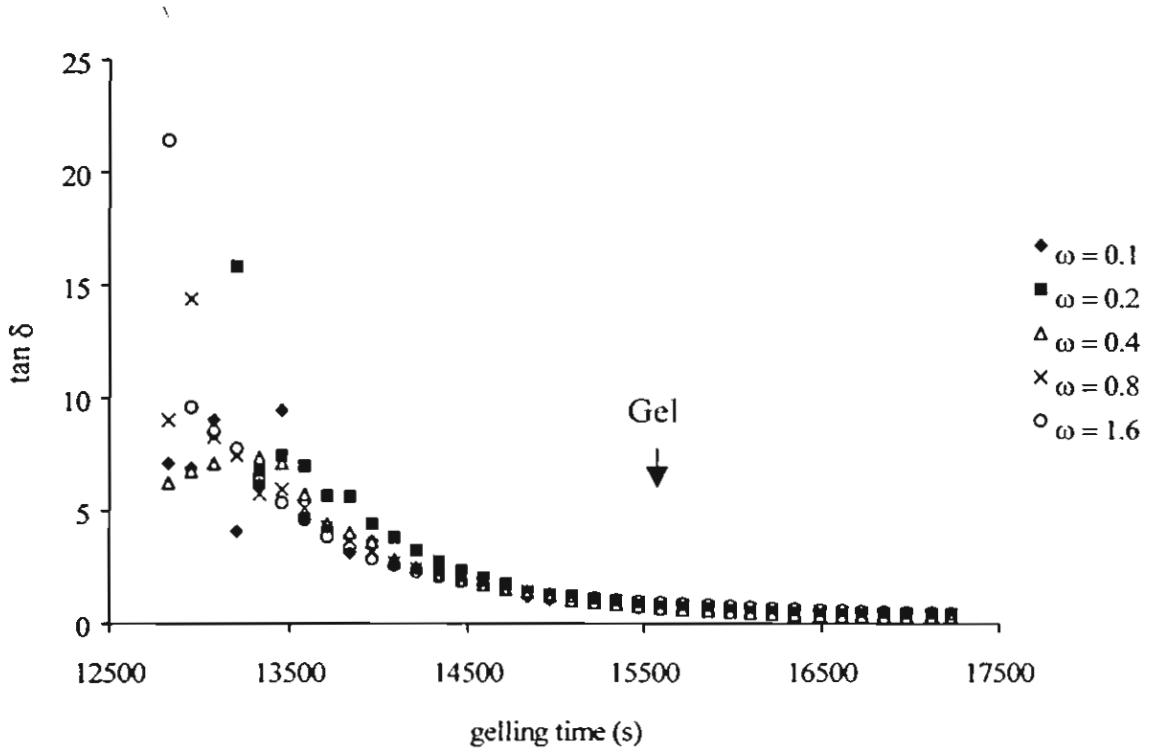

Figure 4.4 Multi-frequency plot of tanδ vs. gelling time of 150% w/v silatrane complex hydrolyzed in water at T = 40°C.

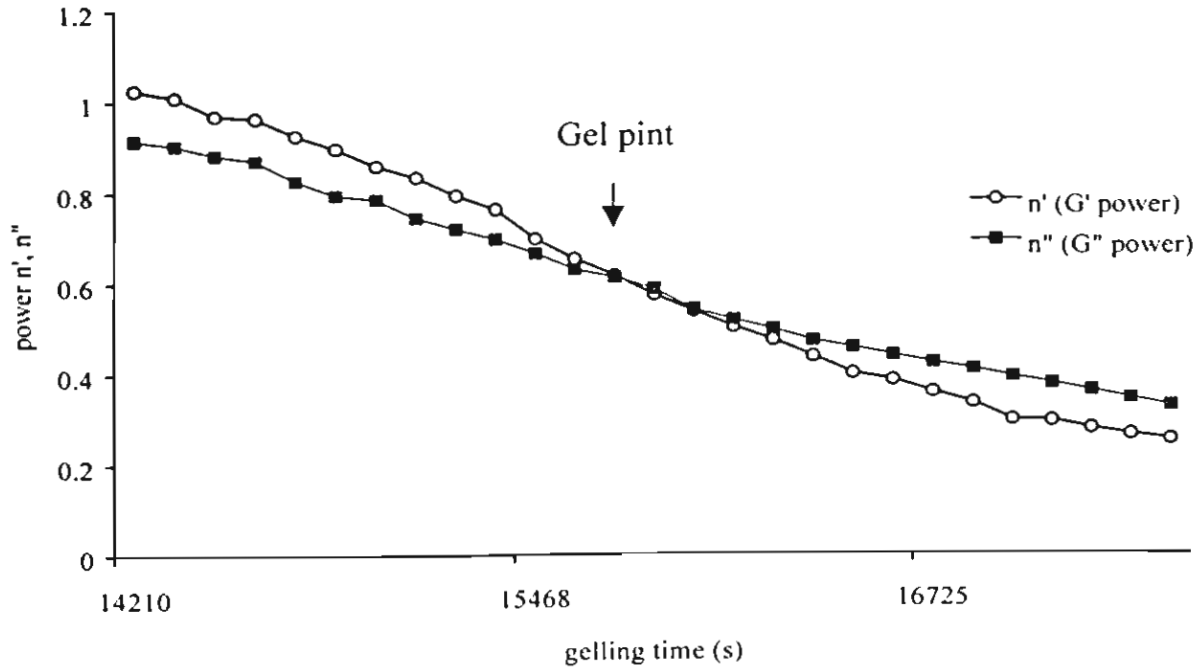

Figure 4.5 The plot of power-law exponent n' and n" vs. gelling time of 150% w/v silatrane complex hydrolyzed in water at T = 40°C.

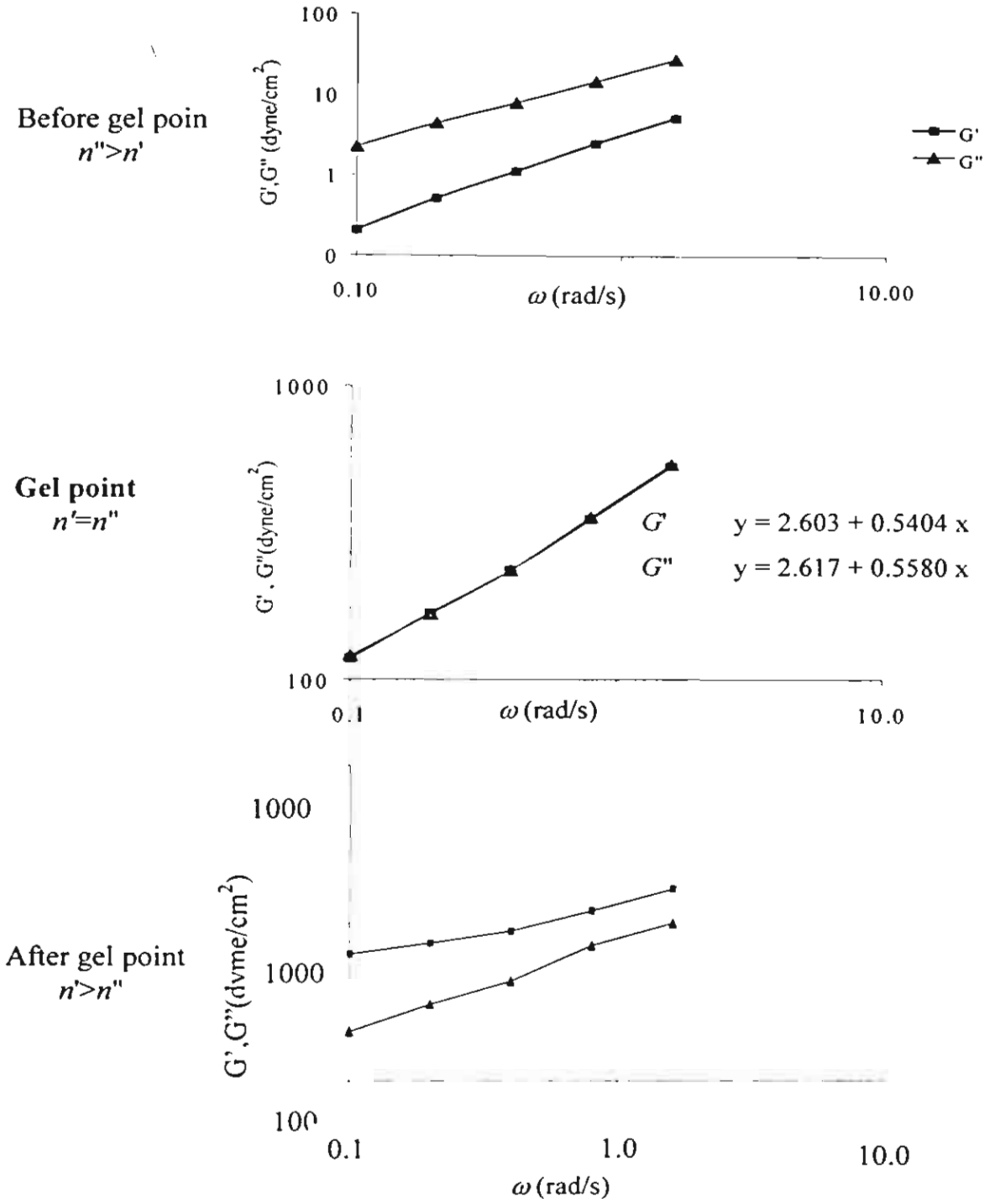

Figure 4.3 The relationship of log G' and log G" vs. log frequency of 150% w/v silatrane complex hydrolyzed in water at T = 40°C.

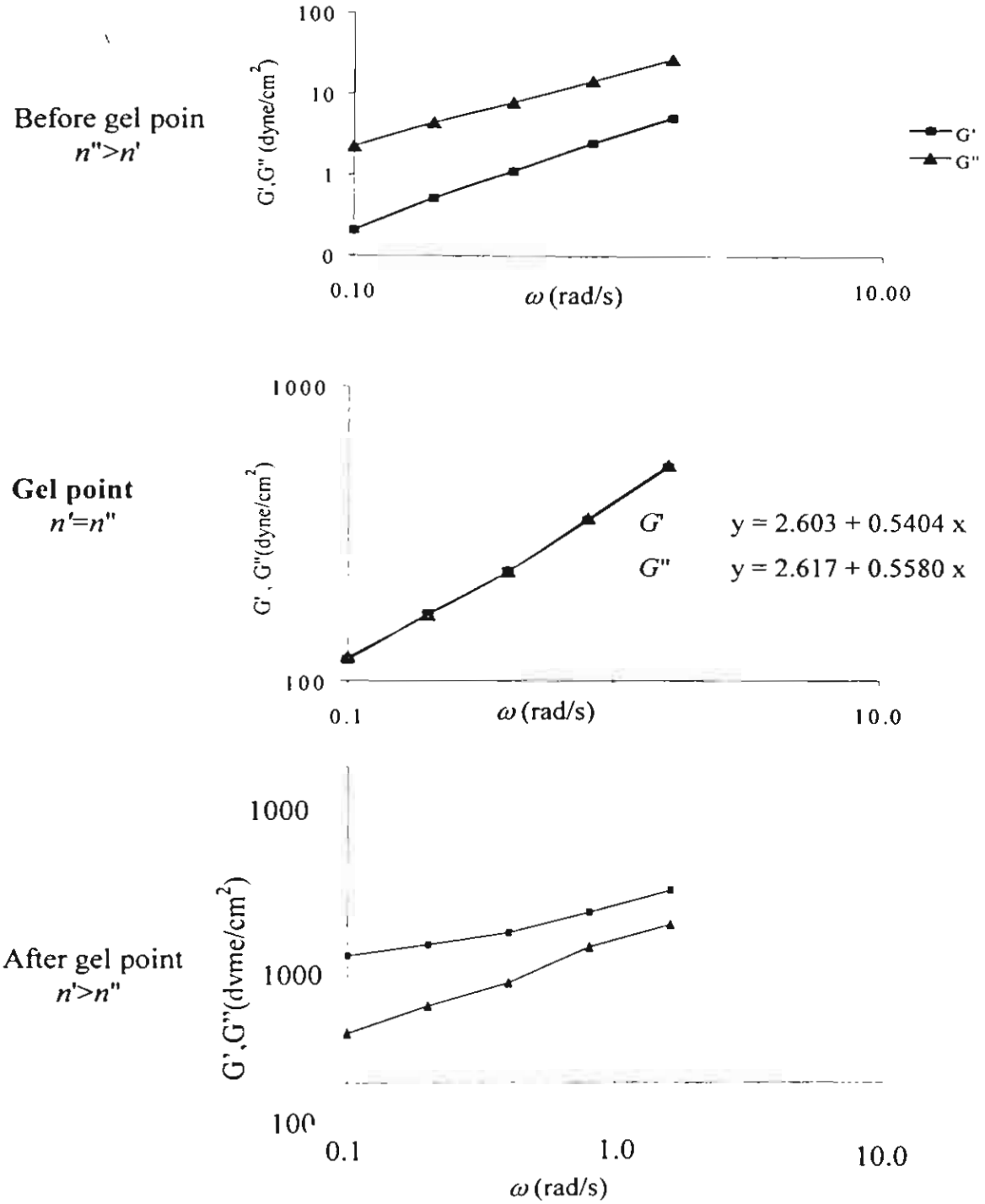

Figure 4.3 The relationship of log G' and log G" vs. log frequency of 150% w/v silatrane complex hydrolyzed in water at T = 40°C.

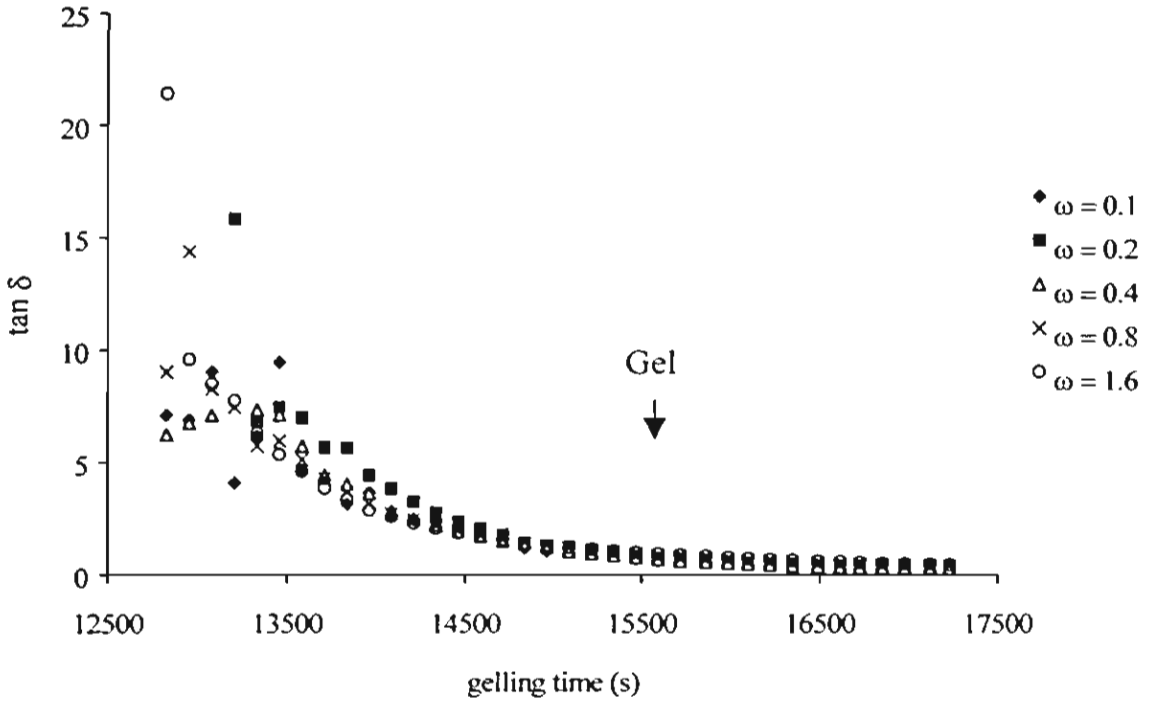

Figure 4.4 Multi-frequency plot of tanδ vs. gelling time of 150% w/v silatrane complex hydrolyzed in water at T = 40°C.

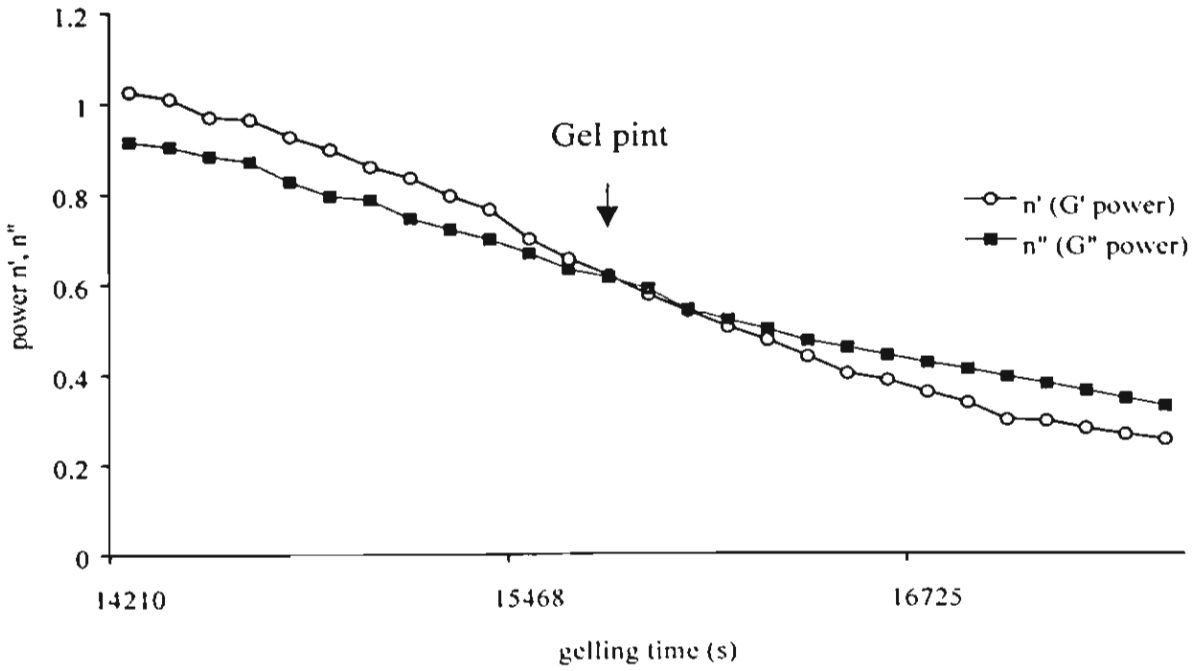

Figure 4.5 The plot of power-law exponent n' and n" vs. gelling time of 150% w/v silatrane complex hydrolyzed in water at T = 40°C.

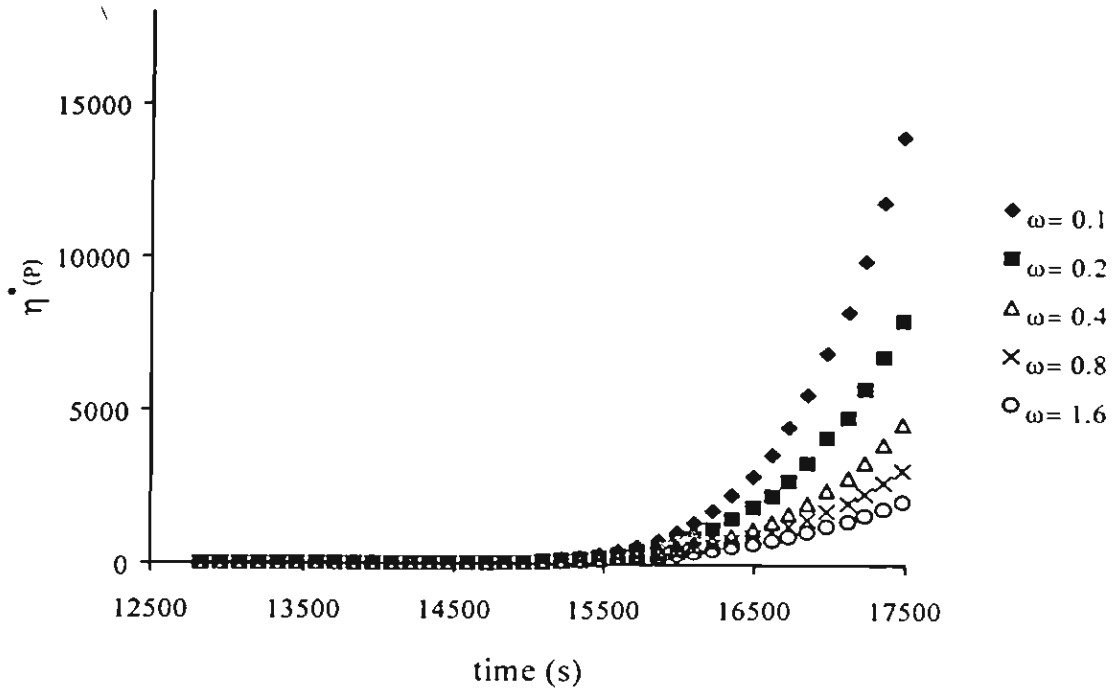

Figure 4.6 Complex viscosity (η^*) at different frequency plotted vs. gelling time of 150% w/v silatrane complex hydrolyzed in water at T = 40°C.

Table 4.3 Viscoelastic properties at the sol-gel transition of polysilatrane.

Solvent	Temperature(°C)	Gelling time(s)	$\tan\delta$	n
$MgO + H_2O$	60	4500	1.31	0.55
H_2O	60	6620	1.62	0.75
$MeOH + H_2O$	60	8260	1.20	0.61
$MgO + H_2O$	50	8950	3.02	0.85
H_2O	50	9350	2.24	0.79
$MeOH + H_2O$	50	9560	0.98	0.49
$MgO + H_2O$	40	14567	1.20	0.62
H_2O	40	16200	1.06	0.53
$MeOH + H_2O$	40	18892	1.42	0.67

Characterization of pyrolyzed ceramics

Polysilatrane gels produced via hydrolysis in the three solvents at 40 °C were pyrolyzed at various temperatures in the range 200 °C to 800 °C. FTIR spectra are shown in Fig 4.7 and indicate increasing conversion to silica, with increasing temperature such that at 800 °C, essentially pure SiO_2 is

obtained. Thus pure ceramic product can be generated in high yield, using processing temperatures as low as 800 °C. The surface areas of ceramics produced by pyrolysis at 800 °C of gels formed in each of the hydrolysis solvents at 40 °C were determined by the BET method. The results are listed in Table 4.4, and indicate a trend of decreasing surface area with decreasing gel times. At high rates of gelation, it is likely that smaller gel particles are formed, which might lead to smaller pore sizes, and hence higher surface areas in the pyrolysed products. In Fig. 4.8, we show SEM micrographs, taken at a magnification of x7500, of the surfaces of the three pyrolyzed ceramics together with that of the fumed silica starting material. Clearly, sol-gel processing via formation of silatrane complexes has converted the silica from a granular porous solid into a homogeneous microporous glass, with a corresponding increase in surface area from 280 m^2/g to ~ 410 m^2/g. From the micrographs, there appears to be a tendency towards smaller pore sizes with shorter gel times. In particular the ceramic from the MgO hydrolysis solvent has the most finely divided morphology, but shows evidence of contamination by small amounts of precipitated MgO on the surface.

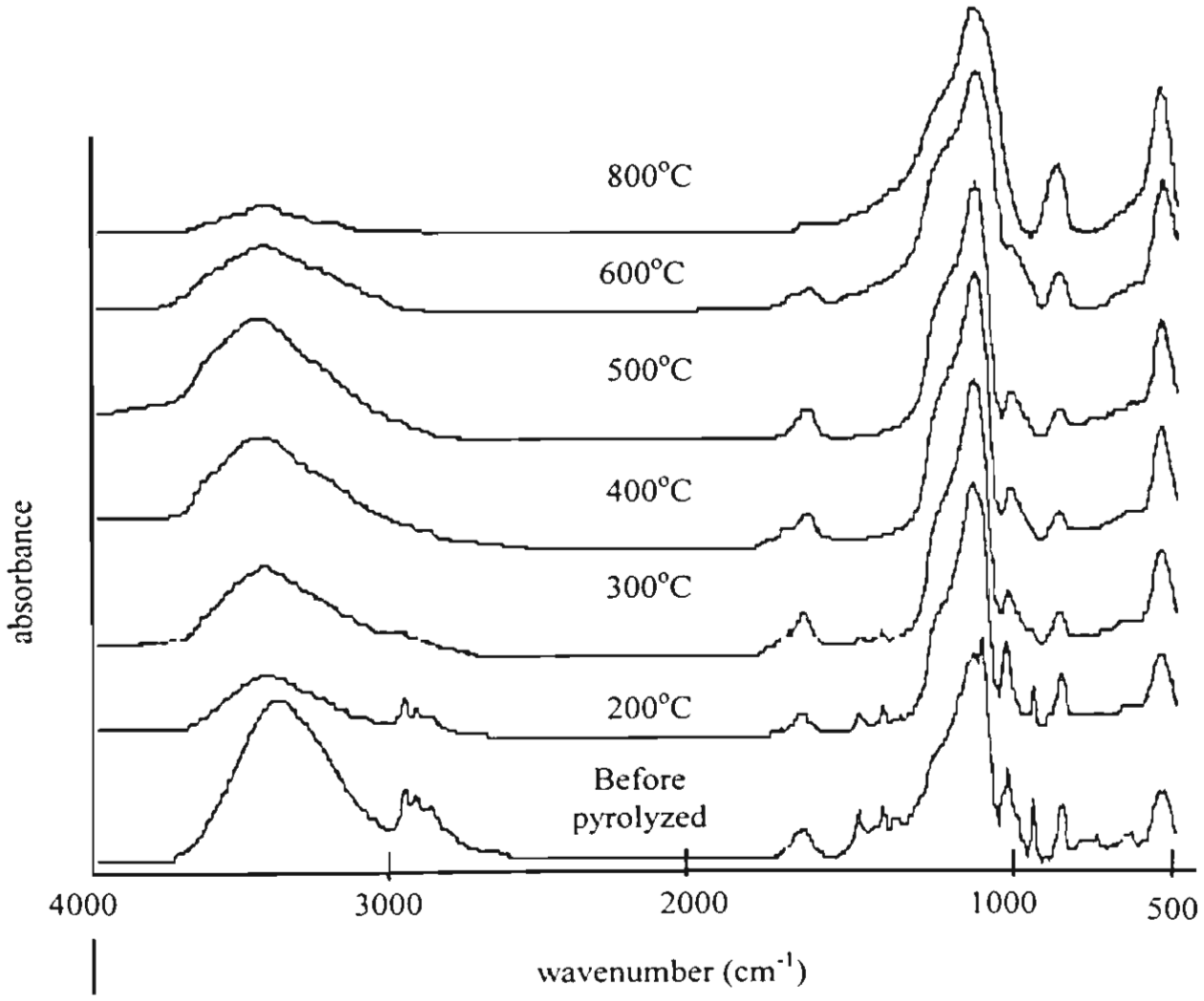

Figure 4.7 FTIR spectra of the pyrolyzed polysilatrane gel at different temperatures.

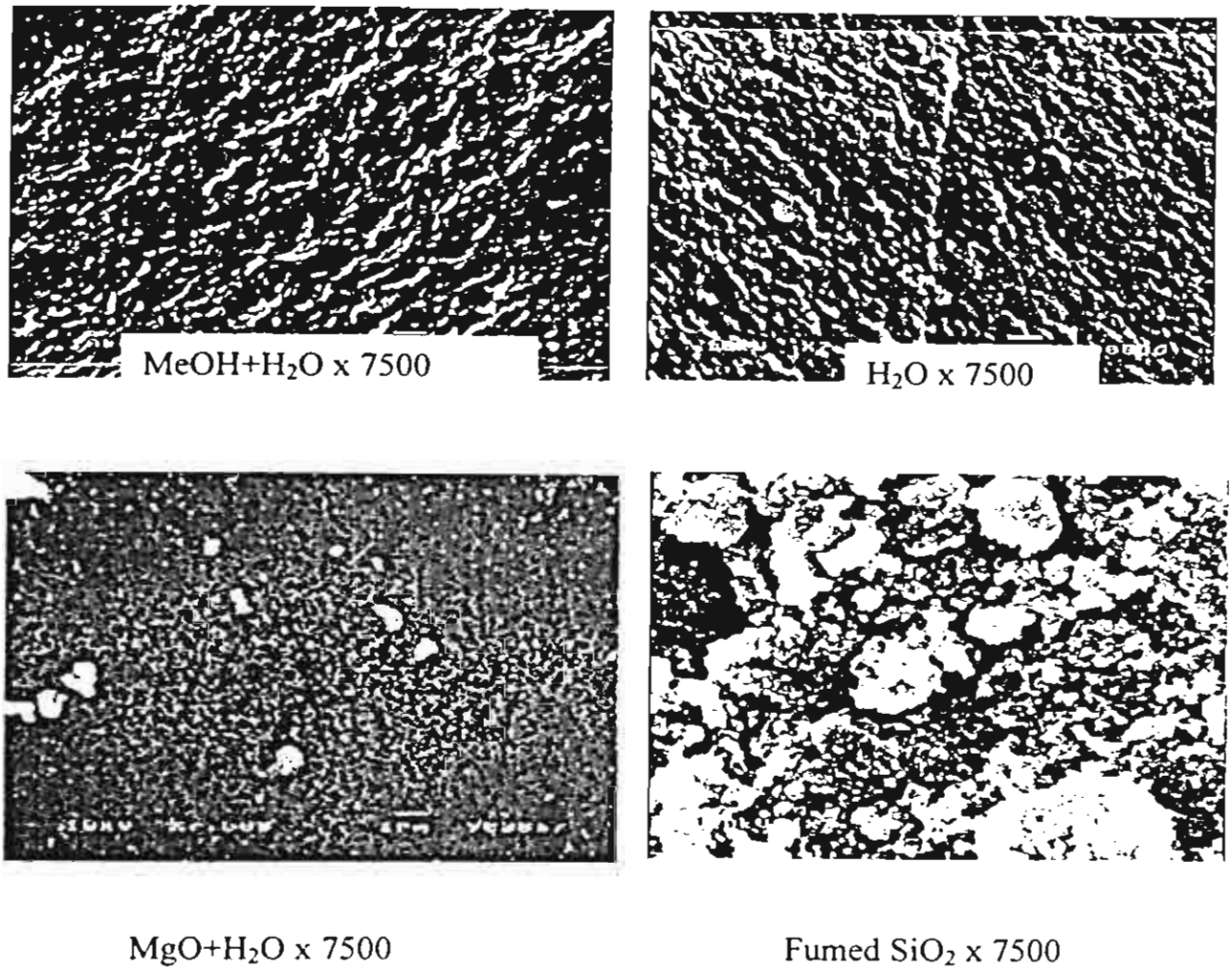

Figure 4.8 SEM micrographs of pyrolyzed polysilatrane hydrolyzed with various solvents, at 800°C, and heating rate of 10°C/min as compared with fumed SiO_2 with magnification of 7500.

Table 4.4 Surface area of polysilatrane gel pyrolyzed at 800°C

Gel	Surface area (m^2/g)
Hydrolyzed MgO+ H_2O	417
Hydrolyzed H_2O	401
Hydrolyzed MeOH+H_2O	313
Pyrolyzed start from 500°C	414
Pyrolyzed start from room temp.	388

CONCLUSIONS

The optimal reaction mixture for silatrane synthesis is one with equimilar amounts of TIS and SiO_2 in the presence of 5 mol% of silica. The optimum vacuum distillation temperature is 180 °C. After 12 hours under these conditions, most of the solvent is removed, and the monomer (M = 277) is largely converted to the dimer with M = 492. Gelation of the silatrane complex formed under these conditions is achieved by hydrolysis under ionic conditions. Pyrolysis of the gels at 800 °C produces a homogeneous microporous glass. Glass formed under more ionic conditions (MgO/H_2O) has the smallest pores and largest surface area, but suffers from contamination by precipitated MgO.

RRFERENCES

1. Saegusa, T. and Chujo, Y., "Organic Polymer Hybridgs with Silica Gel Formed by Means of the Sol-Gel Method", *Advance Polymer Science* 1992, *100*, 11.
2. Varshneya, A., *Fundamentals of Inorganic Glassmaking* 1994, Boston:Academic Press.
3. Iler, R., *The Chemistry of Silica* 1979, NewYork: John Wiley & Sons.
4. Hencsei, P. and Parkanyi, L., "The Molecular Structure of Silatranes", *Review Silicon, Germenium, Tin Lead Compound* 1985, *8(2)*, 191.
5. Bickmore, C., Hoppe, M. and Laine, R., "Processable Oligomeric and Polymeric Precursors to Silicate Prepared Directly from SiO_2, Ethylene Glycol and Base", *Material Research Society Symposia Processing* 1992, *249*, 81.
6. Piboonchaisit, P., Wongkasemjit, S. and Laine, R., "A Novel Route to Tris(silatranyloxy-*i*-propyl)amine Directly from Silica and Triisopropanolamine", *ScienceAsia, J.Sci.Soc. Thailand* 1999, *25*, 113.
7. Winter, H. and Chambon, F., "Analysis of linear viscoelasticity of a crosslinking polymer at the gel point", *J. Rheol.* 1986, *30*, 367.
8. Muthukumar, M. and Winter, H., "Fractal dimension of a crosslinking polymer at the gel point", *Macromolecules* 1986, *19*, 1284.
9. Hodgson, D., Qun, Y. and Amis, E., "Dynamic viscoelasticity during thermoreversible gelatin gelation", *J. Non-Crst. Solids* 1991, *131-133*, 913.
10. Muller, R., Gerard, E., Dugand, P., Rempp, P. and Gnanou, Y., "Rheological characterization of the gel point:A new interpretation", *Macromolecules* 1991, *21*, 532.
11. Izuka, A., Winter, H. and Hashimoto, T., "Molecular weight dependence of viscoelasticity of polycaprolactone critical gels", *Macromolecules* 1992, *25*, 2422.
12. Hsu, S. and Jamieson, A., "Viscoelastic Behavior at the Thermal Sol-Gel Transition of Gelatin", *Polymer* 1993, *34*, 2601.
13. Lin, Y., Matlin, D., Chien, J. and Winter, H., "Dynamic mechanical measurement of crystallization-induced gelation in thermoplastic elastomeric poly(propylene)", *Macromolecules* 1991, *24*, 850.

14. Muthukuma, M., "Screening effect on viscoelasticity near the gel point", *Macromolecules* 1989, 22, 4656.

15. Roy, R., "Gel route to homogeneous glass preparation", *J. Amer. Cer. Soc.* 1969, 344.

16. McCarthy, G. and Roy, R., "Gel route to homogeneous glass preparation II, Gelling and desiccation", *J. Amer. Cer. Soc.* 1971, 639.

CHAPTER V
SOL_GEL PROCESSING OF ALUMATRANE

ABSTRACT

Alumina gels were prepared by the sol-gel method using alumatrane or tris (alumatranyloxy-*i*-propyl)amine as precursor. Alumatrane are aminoalkoxide derivatives of aluminium synthesized directly from the reaction of inexpensive and readily available compounds, aluminium hydroxide and triisopropanolamine, via the one step process. Sol-gel process parameters, such as gelation time, were correlated to variables of the initial stage of the process, such as pH, temperature of hydrolysis and water/alkoxide ratio. The sol-gel transition of alcoholic alumatrane solutions was monitored by multiple waveform rheological measurements. The gelation time could be determined from the evolution of the storage (G') and loss (G'') moduli versus time at different frequencies using the Winter Chambon criterion (convergence of the loss tangents at the gel point). Increasing pH values, hydrolysis ratio and/or temperature accelerates the kinetics of hydrolysis-condensation reactions and thus reduced the gelation time. The gelation times at various temperatures were used to calculate apparent activation energy of the cross-linking leading to the gelation, which was found to be approximately 139 kJ mol^{-1} and independent of hydrolysis ratio. Alumina materials prepared from the heat treatment of obtained gel at 500°C were analyzed using X-ray diffraction and the BET method.

INTRODUCTION

Alumina materials have a wide range of applications in a great number of industrial areas, particularly in catalysis, membrane separation processes, catalytic membrane reactors, adsorbent, composite, coating, fiber, electronic and optic fields.[1-7] Alumina prepared by sol-gel process is frequently used in such areas. In the development of soft chemistry, the sol-gel process is considered to be the most practical method for the synthesis of inorganic oxides. This process usually involves the hydrolysis and condensation of various metal alkoxide molecules under controlled conditions to form metal-oxygen-metal bridging units. In many cases the metal alkoxide precursors are very sensitive to water and therefore cannot be controlled the hydrolysis reaction.[8-9] Generally, the aluminium alkoxides, such as aluminium *sec*-butoxide and aluminium isopropoxide, are used to prepare alumina by sol-gel method.[10-12] However, these commercial precursors are expensive and aluminium *sec*-butoxide can be rapidly hydrolyzed to give the hydrolyzed products dispersed in 2-butanol.[13-17]